Title
Individual differences in white matter integrity: Linking brain structure to cognition in children and adults

Author
Whitaker, Kirstie

Publication Date
2012

Peer reviewed|Thesis/dissertation

Individual differences in white matter integrity: Linking brain structure to cognition in children and adults

by

Kirstie Jane Whitaker

A dissertation submitted in partial satisfaction of the
requirements for the degree of
Doctor of Philosophy
in
Neuroscience
in the
Graduate Division
of the
University of California, Berkeley

Committee in charge:
Professor Silvia A. Bunge, Chair
Professor Jack L. Gallant
Professor William J. Jagust
Professor Qing Zhou

Fall 2012

Abstract

Individual differences in white matter integrity:
Linking brain structure to cognition in children and adults

By

Kirstie Jane Whitaker

Doctor of Philosophy in Neuroscience

University of California, Berkeley

Professor Silvia A. Bunge, Chair

For disparate brain regions to communicate efficiently action potentials must be transmitted relatively long distances along myelinated axons, which make up the brain's "white matter". These connections are fundamental for the generation of complex cognition. A single cortical region is not sufficient—the human brain must work as a network, with the billions of neurons interacting together to perform the necessary computations. In my graduate work, presented in this dissertation, I sought to explain the variability in cognitive behavior with individual differences in white matter microstructure. The overarching goal was to further our understanding of the mechanisms through which structural connections in the brain underlie complex cognition in children and adults.

I used diffusion tensor imaging, a type of magnetic resonance imaging that is sensitive to white matter microstructure, to quantify *in vivo* the maturation of white matter in children and adults. I first motivate the need to study the individual differences in white matter integrity and their predictive value on cognitive behavior in chapter one. I then describe four experiments that investigate various aspects of this connection. In chapter two, I first describe the age related changes in brain and behavior through childhood and adolescence, and then use longitudinal data to highlight the additional explanatory power of how *within-person* measures of change (in brain and cognitive ability) over time are linked. In chapter three, I demonstrate the mediation of the relationship between white matter integrity (WMI) and reasoning ability by cognitive processing speed in typically developing children.

In chapter four, I show the WMI differences between two groups of adults who have experienced different perceptual environments through development (synesthetes and non-synesthetes) and demonstrate a correlation between vividness of visual imagery and the WMI of the synesthetic brain. Finally, in chapter five, I explain the effects of short term cognitive training on WMI . After only three months of undergoing an intensive reasoning training program we saw evidence of cellular reorganization in the white matter of healthy young adults. I conclude by summarizing the major contributions of the work in this dissertation and discuss possible future directions based on the results of my graduate research.

Dedication

For my Granny May, who passed away in 2006, and would have been so proud. I'm sorry I'm not able to show you this thesis in person, although it may be a blessing in disguise: we would never have heard the end of it.

Acknowledgements

This thesis would not exist without the following teams:

My co-authors: None of my papers have fewer than three authors, and I'm proud of that fact. I'm glad that my work in graduate school has been with the support of others, and I'm happy that I have provided that support in exchange. We are greater than the sum of our parts, and we can create so much more when we work together. I can only hope that these collaborations continue through my career, and that they are only the first of many more to come.

My committee: Jack Gallant, Bill Jagust, Qing Zhou and, most importantly, my supervisor, Silvia Bunge, who has devoted countless hours to nurturing my development as a scientist over the last five years. Each member of my thesis committee has supported that learning curve through graduate school with their time and expertise. I am eternally grateful for everything I have learned from them.

My funding: The Fulbright Commission has opened so many doors and has changed me in fundamental ways. I return to the United Kingdom a better scientist, a more open minded individual and with a broader perspective on life. I have had experiences I could never have imagined though this exchange: riding through California every year with 3,000 best friends on AIDS/Lifecycle, seeing the beauty of the United States and learning its history, engaging with the political legacy of UC Berkeley, and being inspired to embrace our differences while simultaneously recognizing (recognising?) the similarities between humans of all creed and color.

My friends: particularly those in the Neuroscience graduate program. I've never been more inspired than after I've heard these exceptional people present their work. I'm so glad to know the leaders of tomorrow. Whether as scientists or in the multitudes of jobs they may join, the graduates of the Helen Wills Neuroscience Graduate Program will affect positive change everywhere they go. I have learned so much from them, and they have supported me through the hardest five years of my life.

And lastly, my family: nothing points out what is important in life better than losing the person you love most in the world. I have been so proud of the support my family has shown me throughout my time in California, thousands of miles away. The morning phone conversations as I walk into school were mundane, and life saving at the same time.

Thank you to everyone; I could never have completed this journey without you.

Table of contents

Chapter 1: Introduction 1

Chapter 2: Longitudinal changes in white matter microstructure predict gains in reasoning ability 5

2.1 Introduction 5

2.2 Results 7

2.3 Discussion 10

2.4 Methods 11

Chapter 3: White Matter Maturation Supports the Development of Reasoning Ability through its Influence on Processing Speed 15

3.1 Introduction 15

3.2 Methods 17

3.3 Results 20

3.4 Discussion 21

3.5 Conclusion 23

Chapter 4: Global differences in the white matter of grapheme-color synesthetes correlate with the vividness of visual imagery 24

4.1 Introduction 24

4.2 Results 26

4.3 Discussion 29

4.4 Conclusion 32

4.5 Methods 32

Chapter 5: Experience-dependent plasticity in white matter microstructure: Reasoning training alters structural connectivity 35

5.1 Introduction 35

5.2 Methods 37

5.3 Results 40

5.4 Discussion 44

Chapter 6: Conclusion 48

References 50

Chapter 1: Introduction

Author contribution statement

Kirstie Whitaker: Wrote the manuscript. The contributions by co-authors in later chapters are acknowledged in place.

For disparate brain regions to communicate efficiently action potentials must be transmitted relatively long distances along myelinated axons, which make up the brain's "white matter". These connections are fundamental for the generation of complex cognition. A single cortical region is not sufficient—the human brain must work as a network, with the billions of neurons interacting together to perform the necessary computations. In my graduate work, presented in this dissertation, I sought to explain the variability in cognitive behavior with individual differences in white matter microstructure. The overarching goal was to further our understanding of the mechanisms through which structural connections in the brain underlie complex cognition in children and adults.

White matter microstructure can be investigated *in vivo* using diffusion tensor imaging (DTI). As water diffuses, it follows the path of least resistance, and therefore preferentially moves along axons, particularly for myelinated axons in a coherent fiber tract (Beaulieu, 2002; Assaf & Pasternak, 2008). Diffusion-weighted magnetic resonance imaging is sensitive to the direction of water movement. After fitting this movement to a tensor model, several measures are commonly extracted that provide information about the white matter microstructure. Fractional anisotropy (FA), a scaled ratio of the propensity of water to diffuse along the axon (parallel diffusivity, λ_1) versus across it (perpendicular diffusivity, λ_{23}), is a measure of white matter coherence (Basser, 1995; Pierpaoli & Basser, 1996) while mean diffusivity (MD) is the average of diffusion in all three orthogonal directions. Together, these tensor measures provide complementary information about the cells present in a region of white matter, commonly referred to as the white matter integrity (WMI).

Although histological studies are capable of examining myelinated axons in exquisite detail (Yakovlev & Lecours, 1967), they have important limitations for examining the relationship between white matter integrity and cognition since these studies cannot be conducted in the living brain. As such, it is difficult to associate levels of myelination in *post mortem* tissue with differences in cognitive abilities *across* individuals and impossible to examine how myelination *within* an individual supports the complex cognition.

The importance of studying individual differences between people (and within the same person at different times) cannot be overstated. Individual difference psychology is strongly grounded in the indisputable fact that no two people are alike and yet no two people are entirely different. The goal of collecting data from a group of study participants is to generalize our findings to a larger population. While many studies collapse across the differences between participants to look for a common behavior, it was my goal in graduate school to highlight these differences and investigate the continuum of white matter integrity and cognitive ability.

Conducting individual difference statistical analyses is challenging. There is a necessary balance between assuming certain similarities between participants (otherwise there would be no

generalization to a larger population) and focusing on one measure of interest. Statistical power is compromised when we try to capture all of the differences between people in just a handful of measures. This thesis describes four experiments which focus on different behavioral measures, but all investigate the predictive power of white matter integrity in the brain. All four studies were carefully designed to maximize the power of the specific hypotheses they sought to test: the developmental cohorts (chapters 2 and 3) utilized large subject populations over a wide age range, and the adult cohorts (chapters 4 and 5) carefully matched two groups of participants so that correlations were not performed over two extremely different data sets.

Over the last five years, I have worked on the Neurodevelopment of Reasoning Ability (NORA) project. We have collected behavioral data from 201 children and adolescents between 6 and 20 years of age, and acquired magnetic resonance imaging (MRI) data from 156 of this group. Of this cohort we have acquired longitudinal behavioral data from 120 participants and 65 have been scanned twice. The NORA data set will continue to facilitate many more exciting analyses on the predictive value of brain and behavior, within the same participants over time, for years to come.

The fundamental question motivating the NORA study concerns the brain mechanisms that underlie the development of reasoning ability (RA). Reasoning ability (alternately known as fluid reasoning or visuo-spatial reasoning) is integral to theories of human intelligence and is the strongest predictor of mathematics achievement between ages 5 and 19 (Taub, Keith, Floyd, & Mcgrew, 2008). RA emerges at around the second or third year of life, improves gradually over childhood and adolescence, and peaks in the early twenties. The acquisition of reasoning ability is thought to serve as a scaffold that allows a child to acquire other cognitive abilities, such as complex spatial, numerical, or conceptual relations.

White matter follows a very similar trajectory of development to that of RA, with both brain and behavior increasing at a decreasing rate, and peaking at around 25 years of age (Ferrer & McArdle, 2004; Lebel, Walker, Leemans, Phillips, & Beaulieu, 2008). Reasoning is such a complex ability that it is very unlikely that one brain region is responsible for reasoning solely: rather the brain relies on a disparate network of regions working together. For this reason, the level of white matter maturation is a persuasive biological mechanism for predicting RA development.

The first experiment (chapter two) specifically investigates the individual differences within the *same person* over time. In a developmental cohort of 33 children aged 6 to 19 years, my co-authors and I report a positive correlation between the change in FA in a white matter tract connecting left lateral prefrontal cortex (PFC) to left posterior parietal cortex and the participant's gains in reasoning ability over 18 months. The same study shows strong relationships between age, WMI, and RA, however the relationship between changes in WMI in the left lateral-frontoparietal tract (l-FPT) and RA remains even when this developmental relationship is taken into consideration. We conclude that the age-related developmental changes are distinct from the individual within-person relationships between brain and behavior over time.

This study highlights the complex distinction between variables of interest and variables of non-interest. Is the participant's chronological age signal or noise? In almost all cases the answer is

both. Age, while explaining huge amounts of variance in many measures of brain structure, function and behavior, is not a biological mechanism *per se*. However, cognitive abilities themselves may be hierarchically acquired. In chapter three, as part of the same cohort of children 6 to 19 years old, my co-authors and I used structural equation modeling (SEM) to investigate the extent to which the relationship between white matter integrity and RA is mediated by cognitive processing speed. In this study we were interested in the individual differences *between participants* in a cross-sectional cohort.

Our neuropsychological measures of RA and cognitive speed, and our measure of brain structure (WMI), are highly correlated both with each other and with chronological age. We found that processing speed completely mediates the relationship between WMI and RA. In this study, the most parsimonious model was a global measure of white matter integrity (mean FA from white matter across the whole brain) predicting processing speed which in turns predicts RA. Here we show the structure of individual differences in WMI and two measures of cognitive ability in a cross-sectional cohort. The use of SEM, which is infrequently used in neuroimaging studies, allows us to investigate these multi-dimensional relationships in one analysis.

While chapters two and three look at *development*—studying participants who are still in the process of changing—chapter four looks at the differences between two groups of participants: synesthestes and non-synesthetes. Specifically, we studied grapheme-color synesthetes who have had synesthetic experiences from as early as they can remember. These participants see a color associated with each letter of the alphabet. These colors do not change over time, and they are not affected by the color in which the letter is actually written. They are also not the same between synesthetes. Although it is difficult to study conclusively, synesthesia is thought to be caused by a genetic factor (Ward & Simner, 2005), leading synesthetes to experience a different developmental trajectory (as compared with non-synesthetes) from birth. It is typical to refer to the synesthetes in our study as "congenital synesthetes" even though their experiences probably took years to develop.

This study (chapter four) represents the combination of traditional "group differences" analyses and individual difference analyses. In collaboration with Bryan Alvarez, who designed the study, I generated an analysis pipeline which allowed us to investigate, throughout the brain, group differences in measures of WMI, correlations with the vividness of visual imagery (VVI), and the interaction of group membership (synesthete vs. non-synethete) and VVI.

We found widespread differences in WMI throughout the brain between synesthetes and non-synesthetes, as well as a correlation between WMI in the synesthetic brain and VVI. VVI itself is not exclusive to the synesthetic experience, although synesthetes had, on average, more vivid imagery when compared to non-synesthete controls. However, it was only in the white matter of our cohort of synesthetes that we found the relationship between individual differences in VVI and WMI. An analysis of the mode of anisotropy, a recently developed measure of the diffusion tensor (Ennis & Kindlmann, 2006), revealed that these differences were likely due to the presence of more crossing pathways in the brains of synesthetes. As white matter became less coherent, and thus more decussated, self-reported visual imagery became more vivid, but only for synesthetes.

Finally, chapter five investigates the dynamic nature of the relationship between brain and behavior. In collaboration with Allyson Mackey, who designed the study, I applied the analysis methods I had developed for the preceding studies, to a study of white matter changes as a result of reasoning training. This study combined many of the aspects which were investigated separately in the first three studies: we studied the same participants over time, albeit over a shorter time scale (three months), and looked for both group differences and individual differences with performance on the Law School Admissions Test (LSAT) within the trained group.

My co-authors and I found that, as a result of studying for the LSAT, two separate measures of white matter integrity changed: perpendicular diffusivity in white matter connecting frontal cortices, and in mean diffusivity within frontal and parietal lobe white matter. These changes were significantly larger than the changes between time points for a set of control participants who were matched for age, gender and intelligence quotient. Further, participants exhibiting larger gains on the LSAT exhibited greater decreases in MD in the right internal capsule.

Together, the results of these four studies provide an insight into the dynamic relationships between brain structure and cognitive behavior. Specifically, I investigate the ability of the brain to communicate efficiently between disparate brain regions through white matter tracts. Each study invokes an individual differences analysis between brain and behavior and contributes complimentary evidence that the connections in our brains support the development of complex cognitive abilities, and maintain them throughout our life.

Chapter 2: Longitudinal changes in white matter microstructure predict gains in reasoning ability

Author contribution statement

Kirstie Whitaker: Collected MRI data, designed and conducted data analyses and wrote the manuscript
Chloe Green: Supervised behavioral data collection and data management
Emilio Ferrer: Designed the study and wrote the manuscript
Silvia Bunge: Designed the study and wrote the manuscript

2.1 Introduction

The ability to reason about the world, and thus solve problems in novel situations, is integral to human cognitive development and success both in school and later life (Gottfredson, 1997). In fact, reasoning ability (RA) has been suggested to serve as a scaffold that allows a child to acquire other cognitive abilities (Investment Hypothesis; Cattell, 1971, 1987). Neuropsychological studies have demonstrated that improvements in RA occur throughout childhood and adolescence (Ferrer, O'Hare, & Bunge, 2009; McArdle, Ferrer-Caja, Hamagami, & Woodcock, 2002; Richland, Morrison, & Holyoak, 2006; Sternberg & Rifkin, 1979). Importantly, longitudinal studies indicate that RA at one time point can predict later gains in quantitative ability and general academic knowledge (Ferrer & McArdle, 2004).

Functional magnetic resonance imaging (fMRI) studies involving adults have highlighted the activation of lateral prefrontal and posterior parietal cortices when adults engage in various types of reasoning (Braver & Bongiolatti, 2002; Jung & Haier, 2007; Krawczyk, 2012). Researchers have begun to investigate the neural basis of age-related changes through childhood and adolescence in reasoning ability, and their studies point to refinement of the lateral fronto-parietal circuit that supports reasoning (Crone, Wendelken, Donohue, van Leijenhorst, & Bunge, 2006; Dumontheil, Houlton, Christoff, & Blakemore, 2010; Eslinger et al., 2009; Wendelken, O'Hare, Whitaker, Ferrer, & Bunge, 2011).

To characterize the structural changes in the brain that underlie the development of reasoning ability over age, Dumontheil and colleagues (2010) conducted a neuroimaging study on 37 adolescent and young adult females (11-37 years-old). Findings revealed nonlinear changes in LPFC engagement for a reasoning task that were partly accounted for by local changes in gray matter and white matter volume. By contrast, we found that in 85 children 6-18 years old, age-related functional changes in LPFC were not explained by local changes in cortical thickness (Wendelken et al., 2011), but that changing thickness of parietal cortex did impact prefrontal activation. It is a little challenging to interpret changes in cortical thickness as it is almost always a composite measure of receding gray matter and encroaching white matter. In this study we sought to complement these previous studies by specifically studying white matter microstructure. Our goal was to test whether the strength of anatomical connections between LPFC and parietal cortex is a major contributor to age-related changes in reasoning and individual differences in the development of this ability.

In order for LPFC and parietal cortex to communicate effectively with one another, the connections between them must be fast and messages must be sent with high fidelity. These connections are actualized in the brain as action potentials along myelinated axons. Myelin is the fatty sheath that surrounds and insulates these axons, and permits the long-range transmission of information across distributed brain networks. Signals are sent between specialized cortical regions through the white matter (named for the light color of the myelin sheath) and the temporal precision of these signals is paramount to efficient communication (Engel, Fries, & Singer, 2001). Additionally myelin prevents signal degradation over the relatively long distances between distal cortical regions (Catani & Ffytche, 2005).

The development of complex cognition relies heavily on the maturation of these structural connections between cortical regions. Both the thickness and degree of myelination of white matter fiber tracts affect action potential conduction speed (Gutiérrez, Boison, Heinemann, & Stoffel, 1995; Tolhurst & Lewis, 1992; Waxman, 1980). Histological studies have shown changes in myelin through childhood and adolescence, and even into the third decade of life (Benes, Turtle, Khan, & Farol, 1994; Yakovlev & Lecours, 1967). Additionally, recent work using diffusion tensor imaging (DTI, explained in detail in the methods section) has provided an indirect measure of white matter maturation *in vivo* (Lebel & Beaulieu, 2011; Lebel, Walker, Leemans, Phillips, & Beaulieu, 2008). DTI provides an index of the organization, or integrity, of white matter: i.e., the extent to which axons follow coherent pathways, as well as the degree to which these axons are myelinated (Beaulieu, 2002).

While a child's age is both a simple and direct indicator of a child's current stage in the development, it does not provide us any insight in to the underlying biological mechanism(s) that cause the dramatic cognitive gains we see in the first two decades of life. Just as RA increases through childhood and adolescence and plateaus in the mid-20s, so does white matter integrity (WMI) in many regions of the brain. In the current study, we sought to investigate both the similarity of the age-related increases in RA and WMI and the individual differences between children of the same age.

Showing that these two measures of development (brain and behavior) follow similar trajectories is not sufficient to show that they are causally linked. In fact, previous work by Shaw and colleagues (2006) has demonstrated that children with very high intelligence show different developmental trajectories of cortical thickness to those of average intelligence. Their results focus on the timing differences in cortical thickness between groups of children with different intelligence scores and demonstrate the dynamic nature of brain development. From our overall cohort of 103 children and adolescents, we scanned a subset of our participants (n=33) twice, approximately 1.5 years apart, and looked at *within-person* changes in both WMI and RA. We hypothesized that individual differences in the change in these measures of development would correlate. Data from the same participants as two different time points allow us to distinguish between individual differences in absolute value WMI and RA, and how these measures change over time. Here, we used our longitudinal cohort to ask whether the extent to which the brain changes over time predicts gains in RA.

2.2 Results

Behavioral results

Four standardized tests of RA were used to derive an RA factor score for each participant. The high factor loadings, shown in Figure 1, indicate that the four tests all contributed strongly and equally to the RA factor score (Figure 1).

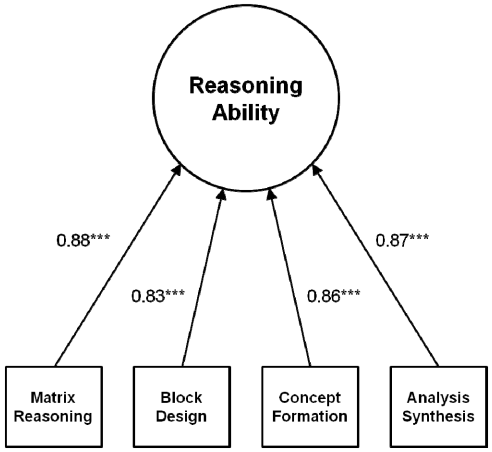

Figure 2.1: A reasoning ability factor score was calculated using a factor analysis of four standardized neuropyschological measures of reasoning: Matrix reasoning, Block Design, Concept Formation and Analysis Synthesis. The factor loadings were strong and each test significantly and equally contributing to the reasoning ability latent variable ($p < 0.001$ for all tests).

To characterize the growth of reasoning from age 6 to 19, we correlated the RA factor scores with each participant's age using a Von Bertalanffy growth equation of the form $RA = \beta_1 + \beta_2 e^{\frac{age}{\beta_3}}$ and robust regression to adjust for within-person correlation (Williams, 2000). Age predicted 65% of the variance in RA ($r2 = 0.65$, $p < 0.001$; Figure 2.2A). While RA is very strongly correlated with age, it does not elucidate the mechanisms underlying the relationship. We therefore sought to identify whether white matter microstructure could provide future insight into these age related changes, or the individual variations which are not explained by age.

DTI results

Given the functional importance of LPFC and posterior parietal cortex, we calculated WMI along the lateral fronto-parietal tract (l-FPT) that connected these two regions. We aimed to replicate previous findings (from different participant populations) that have shown similar developmental trajectories for RA and WMI using data from the same individuals. We fit the same Von Bertalanffy growth model to white matter integrity (as indexed by fractional anisotropy) in the left and right l-FPT, and in whole brain white matter. We found significant

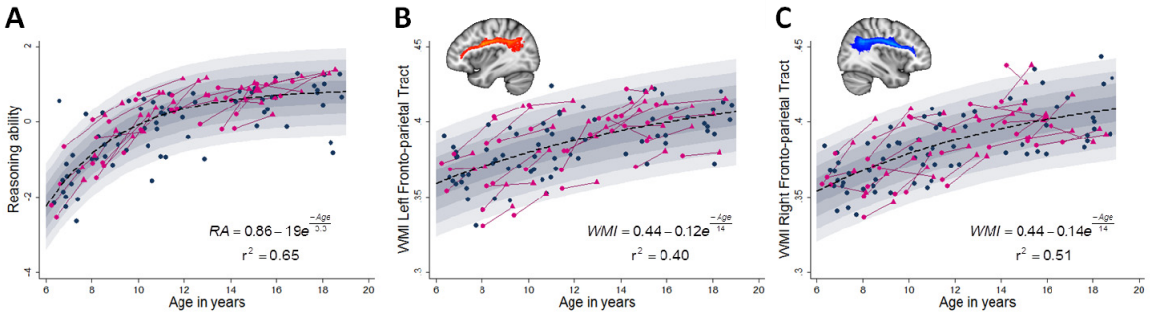

Figure 2.2: Reasoning ability (A), and white matter integrity (indexed by fractional anisotropy, B and C) increase at a decreasing rate through childhood and adolescence. Blue: cross-sectional participants (n = 70), pink: longitudinal participants (n=33). Left (B) and right (C) fronto-parietal tracts created by probabilistic tractography are shown inset.

increases in FA with age in both left and right l-FPT (left: $r^2 = 0.36$, $p<0.001$, Figure 2.2B; right: $r^2 = 0.45$, $p<0.001$, Figure 2.2C) and whole brain FA ($r^2 = 0.40$, $p<0.001$). For each of these regions, and also for RA, a Von Bertalanffy growth equation explained more variance than a linear model.

Given that our longitudinal cohort was a subset of our larger participant pool, we sought to verify that there were no differences in RA or white matter integrity between the cross-sectional and longitudinal groups. For all four regressions, we investigated the distribution of residual variance (the difference between the actual data and the model's predicted value) between three cohorts: cross-sectional only, longitudinal group at time 1, and longitudinal group at time 2.

The cross-sectional and longitudinal groups did not differ at time 1 in terms of RA, but RA was significantly higher in the longitudinal group at time 2 when compared to both their time 1 data ($t(101) = 2.2$, $p < 0.05$) and to the cross-sectional group ($t(101) = 3.7$ $p < 0.01$). This difference is not surprising, given the practice effects inherent in taking the same standardized tests twice. The longitudinal group did not differ in age from the cross-sectional group at either time 1 ($t(101) = 0.61$, $p = 0.27$) or time 2 ($t(101) = 1.46$, $p = 0.07$). The distributions of residual variance from the model fit between the three cohorts did not differ for any of the brain measures ($p > 0.05$ for all t-tests). These results indicate that our longitudinal cohort is a fair and representative sample from our overall study population, and that the practice effects shown in the neuropsychological data are not reflected in the DTI data.

To investigate the predictive power of white matter integrity on the within-person development

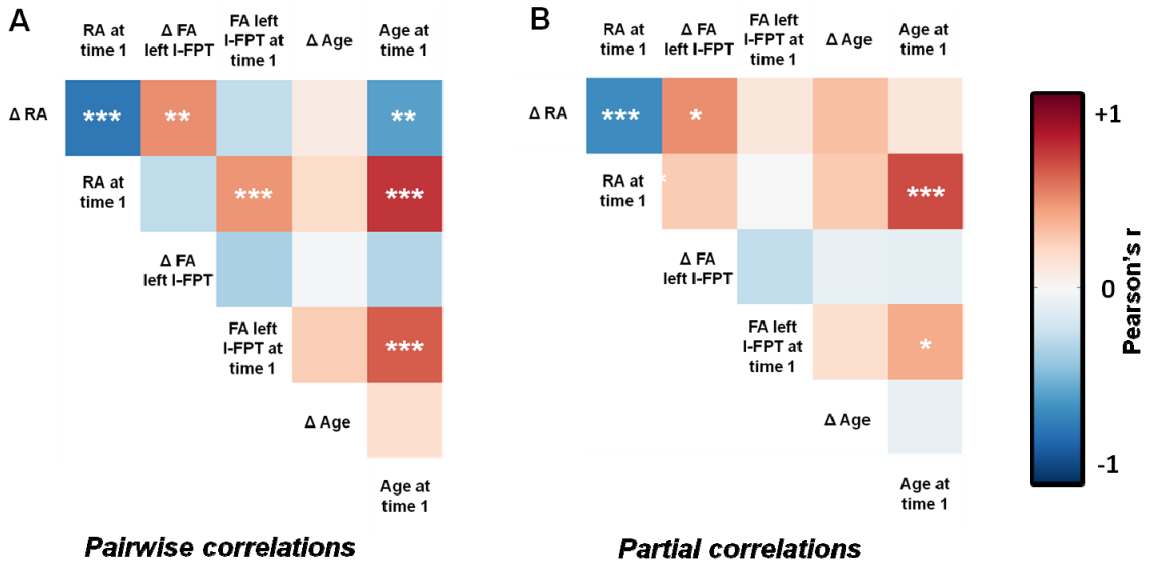

Figure 2.3: Pairwise (A) and partial (B) correlations between variables of interest: change in reasoning ability between scans (Δ RA), RA at time 1, change in FA in the left lateral frontoparietal tract between scans (Δ FA left l-FPT), FA in left l-FPT at time 1, time between scans (Δ Age) and Age at time 1. Positive and negative correlations are shown in red and blue respectively, and significant correlations are marked with astrixes (* $p < 0.05$; ** $p < 0.01$; *** $p < 0.001$).

of RA, we conducted a multiple regression analysis for each white matter ROI. We predicted change in RA with independent variables: RA at time 1, FA at time 1, age at time 1, change in FA, and change in age between scans within our longitudinal cohort. Many of these variables were significantly correlated with each other (pairwise correlations shown in Figure 2.3A). For example, the change in RA between time 1 and time 2 was negatively correlated with RA at time 1 ($r^2 = 0.51$, $p < 0.001$). This relationship fits with the growth model shown in Figure 2.2: RA increases at a decreasing rate, such that high RA is associated with lower gains in RA over time. The negative relationship between change in RA and age at time 1 shows the same negative correlation, for the same reason ($r^2 = 0.29$, $p < 0.01$).

When we look at partial correlations (Figure 2.3B), which can be interpreted as the unique variance explained by a pair of variables, we see that this pattern of decreasing gains in RA with increasing RA or age at time 1 is entirely explained by initial RA ($r^2 = 0.39$, $p < 0.001$). When initial RA is accounted for, age no longer significantly explains any of the variance in RA gains between scans ($r^2 = 0.01$, $p = 0.63$). By design, change in age between scans was not significantly correlated with any of the other variables, either in the pairwise or partial correlational analyses ($p > 0.05$ for all tests).

For both the pairwise and the partial correlations, there is a positive correlation between change in RA and change in FA in the left l-FPT between time 1 and time 2 (pairwise: $r^2 = 0.22$, $p < 0.01$; partial: $r^2 = 0.22$, $p < 0.05$; Figure 3). Here we see a unique explanation of the individual differences in gains in RA from the change in FA of the left l-FPT. This relationship is not replicated in the right l-FPT (pairwise: $r^2 = 0.03$, $p = 0.32$; partial: $r^2 = 0.03$, $p = 0.41$). When change in the whole brain measure of FA is considered, we see a significant positive pairwise correlation with change in RA ($r^2 = 0.14$, $p < 0.01$) but it is not significant when the other explanatory variables (age, FR and initial FA at time 1, and difference in age between scans) are taken into account (partial $r^2 = 0.03$, $p = 0.39$). Thus, we can conclude that gains in RA over 18 months are correlated with FA in the left l-FPT specifically, rather than globally throughout the brain.

Within the longitudinal cohort, age and FA at time 1 are significantly correlated for all three of the white matter regions, even when only the unique variance between these measures is considered (left l-FPT: pairwise $r^2 = 0.35$, $p < 0.001$, Figure 3A, partial: $r^2 = 0.14$, $p < 0.05$, Figure 2.3B; right l-FPT: pairwise $r^2 = 0.44$, $p < 0.001$, partial $r^2 = 0.29$, $p < 0.01$; whole brain: pairwise $r^2 = 0.39$, $p < 0.001$, partial $r^2 = 0.15$, $p < 0.05$). RA and FA at time 1 were also correlated in the pairwise analysis but did not explain unique variance in the partial correlation analysis (left l-FPT: pairwise $r^2 = 0.21$, $p < 0.001$, Figure 2.3A, partial $r^2 = 0.001$, $p = 0.98$, Figure 2.3B; right l-FPT: pairwise $r^2 = 0.21$, $p < 0.001$, partial $r^2 = 0.007$, $p = 0.65$; whole brain: pairwise $r^2 = 0.23$, $p < 0.001$, partial $r^2 = 0.005$, $p = 0.73$).

Finally, we conducted a stepwise regression of all the predictor variables on the change in RA. The best model used RA at time 1 and change in FA of the left l-FPT to explain 60% of the variance in the change in RA. Change in FA explained an additional 9% of the variance in the change in RA, over and above the strong correlation between change in RA and RA at time 1. Performing forwards and backwards stepwise regressions resulted in the same final model.

2.3 Discussion

In our cohort of 103 children between the ages of 6 and 19 years old we see massive improvements in visuospatial reasoning ability and in FA in right and left l-FPT as well as globally throughout the whole brain. Both brain and behavior show an "increasing at a decreasing rate" growth pattern with the steep gains during childhood becoming less substantial in late adolescence. FA in all regions of interest and RA were correlated with each other, but this relationship did not survive when age was taken into account. For our cross-sectional cohort, the individual differences in FA between participants of the same age were not correlated with individual differences in RA.

In order to answer the question of whether it is the change in brain that predicts behavior over time, we turned to our longitudinal cohort, which allowed us to study the *same person* at two time points. Here we were able to disentangle the causality of the relationship between brain and behavior. Despite the strong age-related changes, we found that the amount a person improves in RA is predicted by the amount that their brain changes

In this study, we found that it was changes in FA specifically in the left l-FPT tract that predicted gains in RA; our results were not replicated in the right l-FPT, nor in a measure of whole brain FA. We chose to investigate the tracts connecting LPFC and parietal cortex in both hemispheres because bilateral frontoparietal regions have been shown to be active in fMRI studies of reasoning. However, it is the left hemisphere that has generally shown the most consistent involvement in RA (Braver & Bongiolatti, 2002; Bunge, Helskog, & Wendelken, 2009; Gray, Chabris, & Braver, 2003; Jung & Haier, 2007; Krawczyk, 2012). Taken with evidence that the left hemisphere is actually necessary for successful reasoning (Baldo, Bunge, Wilson, & Dronkers, 2010) our results corroborate the previous literature: the development of the left fronto-parietal connections plays a key role in the development of this integral cognitive ability. This is not to say that the right l-FPT is not involved in reasoning, rather, that the individual differences in its developmental trajectory over time do not correlate with gains in RA. FA in right l-FPT is more strongly correlated with age than FA in the left tract, and it may simply be a limitation of this study that we do not have sufficient statistical power to explain individual differences in white matter integrity over and above the large age effect.

Studies in animals have shown increased FA is related to increased myelination (Blumenfeld-Katzir, Pasternak, Dagan, & Assaf, 2011; Vorísek & Syková, 1997; J. Zhang et al., 2009)and it is very plausible that our results represent myelination in these tracts. Both cross-sectional and longitudinal studies have shown increases in FA though childhood and adolescence (Lebel et al., 2008; Lebel & Beaulieu, 2011) and support the histological finding that myelin continues to develop into the third decade of life (Yakovlev & Lecours, 1967). However, it is important to note that while myelin does affect diffusion (Concha, Livy, Beaulieu, Wheatley, & Gross, 2010; Mottershead et al., 2003), unmyelinated axon membranes do as well (Partridge et al., 2004), and myelin volume and axon counts are very highly correlated (Concha et al., 2010; Schmierer et al., 2007). The extent to which axonal cell membranes also constrain diffusion is unclear. We can conclude from this study that the white matter microstructure is changing, but it is not necessarily the case that myelination is the sole cause. As *in vivo* measures of white matter

development continue to improve, we hope that future studies will improve our understandings of the biological mechanisms underpinning the relationship between RA gains and change in FA.

One potential concern would be that the longitudinal cohort was not representative of our cross-sectional group. However, they did not differ on any of the brain or behavioral measures at their first time point, nor did they fit the age trajectories differently. We are therefore confident that our longitudinal results reflect our study's population fairly. Future work will be needed to investigate the extent to which our findings generalize beyond this sample of children. Additionally, we designed the study such that the time between scans was randomized evenly throughout the age range. Our results showed no correlation for time between scans with any of our dependent measures, further supporting our finding that the observed individual differences in brain and behavioral development are not captured fully by chronological age alone.

Age is a good proxy measure for development, though, and it is difficult to disentangle the massive age related changes that occur in both brain and behavior through childhood and adolescence. All of our variables (WMI in left and right l-FPT and in the whole brain, and RA) correlated with age at time 1, even when other factors were statistically taken into account.. In studying longitudinal data we showed that gains a *particular individual* experienced in RA was correlated with the extent to which their brain changed. In other words, it is the trajectory of development, not just the absolute values, which best explains the within-person changes in brain and behavior. The ability to reason about the world, and thus solve problems in novel situations, is integral to human cognitive development. In understanding the dynamic brain changes which underlie changes in RA over time we move closer to ensuring all children receive the best support for success in later life.

2.4 Methods

Participants

Participants in this study were individuals from the Neural Development of Reasoning Ability (NORA) study, a project designed to examine the behavioral and neural factors that underlie reasoning ability. FMRI data from this cohort has previously been published in Wendelken et al (Wendelken et al., 2011). All participants were screened for neurological impairment, psychiatric illness, history of learning disability and developmental delay. Parents completed the Child Behavioral Check List (Achenbach, 1991) on behalf of their child, and participants who scored in the clinical range for either externalizing or internalizing behaviors were excluded from further analyses (n = 29). All participants and their parents gave their informed assent or consent to participate in the study, which was approved by the Committee for Protection of Human Subjects at the University of California at Berkeley.

Of the 172 children and adolescents who scored in the normal range on the Child Behavior Check List, 70 successfully completed both the behavioral and MRI scan sessions (55 males) on one occasion. These cross-sectional participants ranged in age from 6.3 to 18.9 years (mean 11.8 ± 3.9). An additional 33 participants completed both behavioral and MRI scan sessions at two time points. This longitudinal group had a similar age range to the cross-sectional group: time 1: 6.2 to 16.7 years (mean 11.3 ± 3.2), time 2: 7.6 to 18.6 years (mean 12.9 ± 3.3), with an average of 1.6 years between scans (SD: 0.5 years, range 0.9 to 3.3 years).

Behavioral assessment of reasoning ability

Reasoning ability was assessed using a combination of standardized measures, including the Matrix Reasoning and Block Design sub-tests of the Wechsler Abbreviated Scale of Intelligence (WASI; Wechsler, 1999), and the Analysis Synthesis and Concept Formation sub-tests of the Woodcock-Johnson Tests of Achievement (Woodcock, Mather, & McGrew, 2001). Matrix Reasoning, modeled after the traditional test of fluid reasoning Raven's Progressive Matrices (Raven, 1938), measures the ability to select the geometric visual stimulus that accurately completes an array of stimuli arranged according to one or more progression rules. Block Design measures the ability to arrange a set of red-and-white blocks in such a way as to reproduce a 2-dimensional visual pattern shown on a set of cards. Analysis Synthesis measures the ability to analyze the components of an incomplete logic puzzle and to determine and name the missing components. Concept Formation measures the ability to identify and state the rules for concepts when shown illustrations of both instances and non-instances of the concept. All tests are reported to have very high internal consistency and test-retest reliability, ranging from .94 to .95 (McArdle et al., 2002; McGrew, Werder, & Woodcock, 1991). The four measures were combined into a RA factor score using factor analysis in Mplus (Muthen & Muthen, 1998).

Diffusion Tensor Imaging: Overview

DTI constitutes an indirect index of neuronal structure that measures the movement, or "diffusion", of water in the brain with a diffusion-weighted MRI (DW-MRI) scan. DW-MRI detects the movement of protons, which are most commonly found in the brain as part of water molecules. Within the white matter of the brain, water molecules diffuse preferentially along axon bundles because the myelin sheath surrounding the axons impedes the diffusion of water molecules across it. Water molecules that have high directionality are said to exhibit anisotropic diffusion. Within gray matter and cerebrospinal fluid, water molecules can move freely in all directions and thus exhibit isotropic diffusion. Data from a DW-MRI scan can be fitted to a tensor model. The tensor is a multi-dimensional matrix that represents the amount of water diffusion in three orthogonal directions for every voxel in the brain.

Fractional anisotropy (FA) is a widely used measure of white matter coherence. FA is a scalar measure that quantifies how directional diffusion is within a voxel. Voxels containing randomly oriented fibers will have a very small FA (close to 0, reflecting near-isotropic diffusion), while voxels containing coherently oriented fibers will have a large FA (close to 1, reflecting highly anisotropic diffusion). Measurement of these variables can provide clues regarding white matter tract development. When this index is large, the interpretation is that a single axis of movement is possible, with restriction of movement in the accompanying directions (Mori & Zhang, 2006). Increases in myelination around the neurons generally decrease movement perpendicular to the axis of greatest diffusion and thus increase FA. However, it is possible that an increase in FA could also be caused by an increase in the established direction of the neural tracts. Throughout this paper, we refer to FA as a measure of white matter integrity.

Diffusion Tensor Imaging: Data Acquisition and Preprocessing

Brain imaging data were collected at UC Berkeley on a 3-T Siemens Trio TIM MR scanner using a 12-channel head coil with a maximum gradient strength of 40mT/m. DTI data of the -brain was acquired using echo-planar imaging (EPI; TR = 7900 ms; TE = 102 ms; 2.2 mm isotropic voxels; 55 axial slices). Parallel acquisition (GRAPPA) was used with at an

acceleration factor of 2. One non-diffusion-weighted direction and 64 diffusion-weighted directions were acquired with a b-value of 2000 s/mm^2, uniformly distributed across 64 gradient directions. A T1-weighted image was also acquired in each participant for image registration and segmentation (MPRAGE; TR = 2300ms; TE = 2.98ms; 1 mm isotropic voxels).

Analyses were performed using tools from FDT (for Functional MRI of the Brain (FMRIB) Diffusion Toolbox, part of FSL 4.1, Smith, 2002; Woolrich et al., 2009). Brain volumes were skull-stripped using the Brain Extraction Tool (BET, Smith, 2002) and a 12-parameter affine registration to the non-diffusion weighted volume was applied to correct for head motion and eddy current distortions introduced by the gradient coils, and the gradient directions were rotated accordingly. A diffusion tensor model was fit to the data in a voxelwise fashion to generate whole-brain maps of fractional anisotropy.

Each participant's high resolution T1-weighted scan was brain extracted using BET (Smith, 2002) and segmented into grey matter, white matter and cerebral spinal fluid using FAST (FMRIB's Automated Segmentation Tool; (Zhang, Brady, & Smith, 2001) The white matter voxels defined a white matter mask which is an independent definition of white matter voxels in the FA map created from the DTI acquisition. We transformed the mask into the subject's DTI space by applying the inverse of the affine registration of the non-diffusion weighted volume to the high resolution image. Both the registration and calculations of the inverse transform used FLIRT (FMRIB's Linear Image Registration Tool; Jenkinson, Bannister, Brady, & Smith, 2002).

Diffusion Tensor Imaging: Defining tracts of interest

We used probabilistic tractography to define tracts connecting anterior frontal and posterior parietal cortices within each hemisphere. The cortical regions were defined from the Harvard-Oxford cortical atlas (Desikan et al., 2006). The superior lateral occipital complex was used as the posterior parietal region of interest (ROI) and lateral frontal pole ($X > |14|$) as the LPFC ROI. Voxel-wise estimates of the fiber orientation distribution, including the modeling of up to two fibers per voxel, were calculated using BedpostX (Behrens, Berg, Jbabdi, Rushworth, & Woolrich, 2007). Probabilistic fiber tracking was performed for each participant using the following settings: 5000 samples per voxel, maximum 2000 steps, curvature threshold of 0.2, 0.5 mm step length.

Left and right lateral fronto-parietal tracts were computed from anterior to posterior and posterior to anterior. 'Start' and 'stop' masks required tracts to pass through the two relevant cortical regions. Further, exclusion masks were used to restrict probabilistic streamlines to our a priori tracts. The exclusion mask for the fronto-parietal tracts prevented fibers that passed through the mid-sagittal plane, thalamus, basal ganglia, cingulum or insula from being included in our tract. All tractography was conducted in each participant's native DTI space, with masks transformed from standard space using FNIRT (FMRIB's Nonlinear Image Registration Tool; Andersson, Jenkinson, & Smith, 2007a, 2007b).

Upon completion of tractography for each participant, tract images were thresholded to remove voxels through which fewer than 5% of the total number of generated tracts passed. Anterior-to-posterior and posterior-to-anterior tracts were added together and binarized. Individual tract images for all participants were then overlaid on one another in standard space. These tract ROIs were transformed into subject space (using the non-linear warping described above) and white

matter integrity within each tract was defined as the average of every voxel in the FA map that fell both inside the tract ROI and the subject's white matter mask. Whole brain WMI was calculated for each subject as the average of every voxel in the FA map that fell within subject's white matter mask.

Statistical Analyses: Developmental trajectories of brain and behavior
For the three measures of white matter integrity (in left l-FPT, right l-FPT and whole brain) and the reasoning ability factor score, we fit a Von Bertalanffy exponential growth model of the form $y = \beta_1 + \beta_2 e^{\frac{age}{\beta_3}}$ using robust regression to adjust for within-person correlation (Williams, 2000). To verify that our longitudinal cohort was a representative sample of our overall study population, we used a student's t test to compare the distribution of residual variance (the difference between the actual data and the model's predicted value) between three cohorts: cross-sectional group only, longitudinal group at time 1, and longitudinal group at time 2. These tests were conducted for the four developmental trajectories: RA, left l-FPT WMI, right l-FPT WMI and whole brain WMI. All analyses were conducted in Stata 11 (StataCorp, 2009).

Statistical Analyses: Predicting within-person change in reasoning ability
To predict an individual's change in RA over time, we calculated the change in FA within their left and right l-FPT and whole brain white matter separately by subtracting the average value at time 1 from the average value at time 2. We hypothesized that age, RA, and WMI at time 1, along with the changes in age and WMI between scans, would predict change in RA. We calculated pairwise and partial correlations between these 6 variables for each of the three white matter regions. Pairwise correlations simply represent the shared variance between two variables, ignoring the effects of any other factors, while a partial correlation quantifies the unique shared variance after all correlations with other variables have been removed.

We also conducted both forward and backward stepwise regressions between all 10 variables, regressing change in RA between time 1 and time 2 on FA within the 3 white matter ROIs, change in FA within these 3 ROIs, initial age, change in age and initial RA. Variables were included in the final models (added for forward and left in for backwards stepwise regression) if they explained additional variance at the $p < 0.05$ level.

Chapter 3: White Matter Maturation Supports the Development of Reasoning Ability through its Influence on Processing Speed

Author contribution statement

Kirstie Whitaker: Collected MRI data, designed and conducted data analyses and wrote the manuscript
Joel Steele: Designed and conducted data analyses and wrote the manuscript
Chloe Green: Supervised behavioral data collection and data management
Emilio Ferrer: Designed the study and wrote the manuscript
Silvia Bunge: Designed the study and wrote the manuscript

3.1 Introduction

Fluid reasoning represents flexibility of thought – the ability to solve problems and think logically even in new or unfamiliar settings (Cattell, 1987). This core component of cognition is essential throughout the lifespan, and much has been done to measure and study its change over time (Goswami, 1992; Horn, 1991). For a growing child, this facet of emergent intellect serves to scaffold the acquisition of new skills and knowledge (Blair, 2006; Cattell, 1971, 1987). Indeed, prior research indicates that childhood levels of fluid reasoning serve as a strong predictor of later academic achievement and even professional success (Gottfredson, 1997).

What changes in the brain underlie the development of fluid reasoning? Behavioral studies have focused on individual differences in trajectory of change in fluid reasoning over time (McArdle, Ferrer-Caja, Hamagami, & Woodcock, 2002) or on concurrent relations to other facets of cognitive ability (Conway, Cowan, Bunting, Therriault, & Minkoff, 2002; Fry & Hale, 2000; Salthouse, 1996; Salthouse, Babcock, & Shaw, 1991). These studies have pointed to cognitive processing speed as a mediator of fluid reasoning development. The speed and efficiency with which material can be processed, be it external stimuli or self generated thoughts, strongly influences the recruitment of this information for complex cognition (Kail and Salthouse, 1994). Processing speed can be thought of as a bottleneck of fluid reasoning development: the integration of multiple stimuli, which characterizes high-level cognitive processing, cannot occur until these stimuli can be individually understood. Processing speed not only correlates with performance on a broad range of cognitive tasks (Kail & Salthouse, 1994; Li et al., 2004; Salthouse, 2005; Wechsler, 1997), but also with age-related changes throughout the life span (Kail, 1991; Salthouse, 1996).

Cognitive processing, in turn, relies on disparate cortical regions working together as a network. For the network to work optimally, connections must be fast and messages sent with high fidelity. These are manifest in the brain as action potentials along myelinated axons. Myelin is the fatty sheath that surrounds and insulates these axons, and permits the long-range transmission of information across distributed brain networks. Signals are sent between specialized cortical regions through the white matter (named for the light color of the myelin sheath) and the temporal precision of these signals is paramount to efficient communication (Engel, Fries, & Singer, 2001). Additionally myelin prevents signal degradation over the relatively long distances between distal cortical regions (Catani & Ffytche, 2005).

The development of complex cognition relies heavily on the maturation of these structural connections. Both the thickness and degree of myelination of white matter fiber tracts affect action potential conduction speed (Gutiérrez, Boison, Heinemann, & Stoffel, 1995; Tolhurst & Lewis, 1992; Waxman, 1980). Histological studies have shown changes in myelin through childhood and adolescence, and even into the third decade of life (Benes, Turtle, Khan, & Farol, 1994; Yakovlev & Lecours, 1967). Additionally, recent work using diffusion tensor imaging (DTI, explained in detail in the methods section) has provided an indirect measure of white matter maturation *in vivo* (Lebel, Walker, Leemans, Phillips, & Beaulieu, 2008; Lebel & Beaulieu, 2011). DTI provides an index of the organization, or integrity, of white matter: i.e., the extent to which axons follow coherent pathways, as well as the degree to which these axons are myelinated (Beaulieu, 2002).

Previous work in adults has identified significant correlations of white matter integrity (WMI) in the parietal and temporal lobes, and connecting to the left middle frontal gyrus with measures of processing speed (Turken et al., 2008), and Chiang et al (2009) found correlations between fluid intelligence and WMI in the cingulum, optic radiations, superior fronto-occipital fasciculus, internal capsule, callosal isthmus, and the corona radiate. Our goal in this study was to investigate the mediating effect of cognitive processing speed between WMI and fluid reasoning ability. Since both cognitive processing speed and fluid reasoning rely on the coordinated activity of many different brain regions we chose to investigate a global measure of WMI. Additionally, given the strong involvement of lateral prefrontal and parietal cortices in reasoning (Bunge, Wendelken, Badre, & Wagner, 2005; Choi et al., 2008; Crone, Wendelken, Donohue, van Leijenhorst, & Bunge, 2006; Dumontheil, Houlton, Christoff, & Blakemore, 2010; Moseley, Bammer, & Illes, 2002) we investigated WMI in the bilateral white matter tracts connecting these regions.

A number of studies have shown that increased WMI over development is correlated with better cognitive performance (for review see Thomason & Thompson, 2011), and we predict this pattern for fluid reasoning ability too. Currently, it's not clear whether this relation is direct, or whether age-related changes in white matter are indirectly linked to changes in high-level cognitive functions such as reasoning. Increased WMI may be related to improvements in reasoning independent of its relation to processing speed. Alternatively, increased WMI could contribute indirectly to improved reasoning through its effect on processing speed.

In order to investigate this system of relations, all of which are increasing through this age range, we used structural equation modeling (SEM). We assume a causal relationship from brain to behavior, with WMI affecting both fluid reasoning and processing speed, and predict a causal role of processing speed on fluid reasoning. SEM allows us to construct a latent variable for fluid reasoning from four separate neuropsychological tests (explained in detail in the methods section), and we are therefore able to generalize across four distinct instantiations of fluid reasoning and minimize the effect of one specific task. Each relation is tested for its ability to significantly increase the fit of the model, and the models were fit for both global WMI and the bilateral fronto-parietal connection, separately.

Structural equation modeling accommodates the multivariate nature of this data set, which included latent factors and multiple manifest variables. It also facilitates the explicit test of

hypotheses concerning the relation between brain structure and the behavioral data. A recent paper by Salthouse (2011) strongly calls for more sophisticated statistical analyses when investigating the interrelated changes of brain, behavior, and age. Only a handful of studies have used SEM to model the relationship between DTI data and cognitive performance on a battery of tasks (Charlton et al., 2008; Chiang et al., 2009; Voineskos et al., 2010) and, to our knowledge, no prior study has used SEM to investigate the role of white matter maturation in cognitive development through childhood and adolescence.

3.2 Methods

Participants
Participants in this study were individuals from the *Neural Development of Reasoning Ability* (NORA) study, a project designed to examine the behavioral and neural factors that underlie fluid reasoning. FMRI data from this cohort has previously been published in Wendelken et al (2011). All participants were screened for neurological impairment, psychiatric illness, history of learning disability and developmental delay. Parents completed the Child Behavioral Check List (Achenbach, 1991) on behalf of their child, and participants who scored in the clinical range for either externalizing or internalizing behaviors were excluded from further analyses. Of the 172 children and adolescents enrolled in the study who scored in the normal range on the Child Behavior Check List, 103 successfully completed both the behavioral and MRI scan sessions (55 males). They ranged in age from 6.2 to 18.9 years (mean 11.6 ± 3.7). All participants and their parents gave their informed assent or consent to participate in the study, which was approved by the Committee for Protection of Human Subjects at the University of California at Berkeley.

Behavioral measures
Fluid reasoning was assessed using a combination of measures, including the *Matrix Reasoning* and *Block Design* sub-tests of the Wechsler Abbreviated Scale of Intelligence (WASI; Wechsler, 1999), and the *Analysis Synthesis* and *Concept Formation* sub-tests of the Woodcock-Johnson Tests of Achievement (Woodcock, Mather, & McGrew, 2001). *Matrix Reasoning*, modeled after the traditional test of fluid reasoning *Raven's Progressive Matrices* (Raven, 1938), measures the ability to select the geometric visual stimulus that accurately completes an array of stimuli arranged according to one or more progression rules. *Block Design* measures the ability to arrange a set of red-and-white blocks in such a way as to reproduce a 2-dimensional visual pattern shown on a set of cards. *Analysis Synthesis* measures the ability to analyze the components of an incomplete logic puzzle and to determine and name the missing components. *Concept Formation* measures the ability to identify and state the rules for concepts when shown illustrations of both instances and non-instances of the concept. A FR factor score was calculated from a factor analysis of these four tests in Mplus (Muthen & Muthen, 1998).

Processing speed was measured using the *Cross Out* subtest of the Woodcock-Johnson Tests of Achievement (Woodcock et al., 2001). This test measures how rapidly and accurately one can identify, within an array of stimuli, a subset of geometric shapes that match a sample stimulus. All tests are reported to have very high internal consistency and test-retest reliability, ranging from .94 to .95 (McArdle et al., 2002; McGrew, Werder, & Woodcock, 1991).

Diffusion Tensor Imaging: Overview
DTI constitutes an indirect index of neuronal structure that measures the movement, or "diffusion", of water in the brain with a diffusion-weighted MRI (DW-MRI) scan. DW-MRI detects the movement of protons, which are most commonly found in the brain as part of water molecules. Within the white matter of the brain, water molecules diffuse preferentially along axon bundles because the myelin sheath surrounding the axons impedes the diffusion of water molecules across it. Water molecules that have high directionality are said to exhibit *anisotropic* diffusion. Within gray matter and cerebrospinal fluid, water molecules can move freely in all directions and thus exhibit *isotropic* diffusion. Data from a DW-MRI scan can be fitted to a *tensor model* (Figure 3.1a). The tensor is a multi-dimensional matrix that represents the amount of water diffusion in three orthogonal directions for every voxel in the brain.

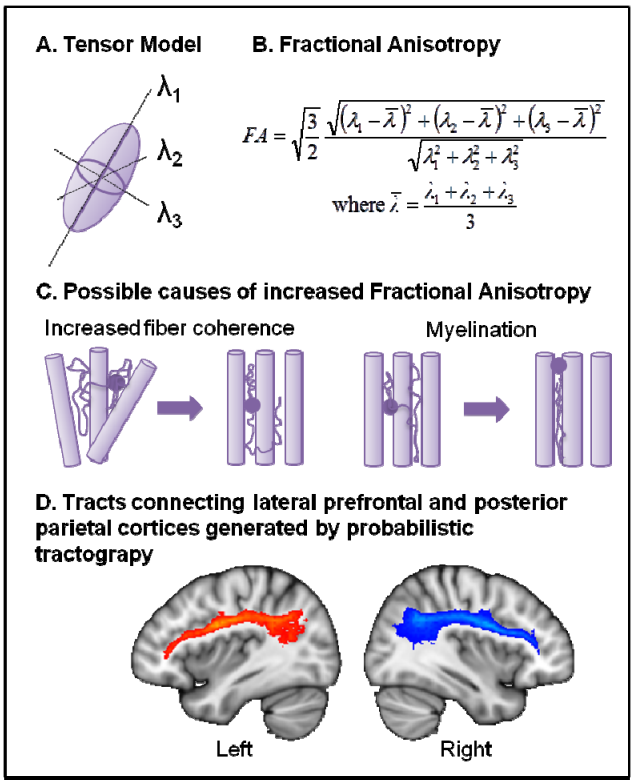

Figure 3.1: Illustration of tensor model and fractional anisotropy. A: Tensor model with eigenvectors along three orthogonal axes. B: Fractional anisotropy (FA) formula. C: Possible mechanisms for an increase in FA. Both increased fiber coherence – either from reorganization of existing axons (shown here) or pruning of axons running in different directions (not shown) –and myelination would result in an increased FA. D: Study specific tracts connecting lateral frontal and parietal cortices in left and right hemispheres generated using probabilisitic tractography.

Fractional anisotropy (FA) is a widely used measure of white matter coherence. FA is a scalar measure that quantifies how directional diffusion is within a voxel (see Figure 3.1b for equation). Voxels containing randomly oriented fibers will have a very small FA (close to 0, reflecting near-isotropic diffusion), while voxels containing coherently oriented fibers will have a large FA (close to 1, reflecting highly anisotropic diffusion). Measurement of these variables can provide clues regarding white matter tract development (see Figure 3.1c). When this index is large, the interpretation is that a single axis of movement is possible, with restriction of movement in the accompanying directions (Mori & Zhang, 2006). Increases in myelination around the neurons generally decrease movement perpendicular to the axis of greatest diffusion and thus increase FA. However, it is possible that an increase in FA could also be caused by an increase in the established direction of the neural tracts.

Diffusion Tensor Imaging: Data Acquisition and Analysis
Brain imaging data was collected at UC Berkeley on a 3-T Siemens Trio TIM MR scanner using a 12-channel head coil with a maximum gradient strength of 40mT/m. DTI data of the -brain was

acquired using echo-planar imaging (EPI; TR = 7900 ms; TE = 102 ms; 2.2 mm^3 isotropic voxels; 55 axial slices). Parallel acquisition (GRAPPA) was used with at an acceleration factor of 2. One non-diffusion-weighted direction and 64 diffusion-weighted directions were acquired with a b-value of 2000 s/mm^2, uniformly distributed across 64 gradient directions. A T1-weighted image was also acquired in each participant for image registration and segmentation (MPRAGE; TR = 2300ms; TE = 2.98ms; 1 mm isotropic voxels).

Analyses were performed using tools from FDT (for Functional MRI of the Brain (FMRIB) Diffusion Toolbox, part of FSL 4.1, Smith, 2002; Woolrich et al., 2009). Brain volumes were skull stripped using the Brain Extraction Tool (Smith, 2002) and a 12 parameter affine registration to the non-diffusion weighted volume was applied to correct for head motion and eddy current distortions introduced by the gradient coils, and the gradient directions were rotated accordingly. A diffusion tensor model was fitted to the data in a voxelwise fashion to generate whole-brain maps of fractional anisotropy.

A white matter mask was created from each participant's high resolution T1-weighted scan, after brain extraction, using FAST (FMRIB's Automated Segmentation Tool; (Zhang, Brady, & Smith, 2001) which segments the brain into grey matter, white matter and cerebral spinal fluid. This mask was transformed into the subject's DTI space by applying the inverse of the affine registration of the non-diffusion weighted volume to the high resolution image. Both the registration and calculations of the inverse transform used FLIRT (FMRIB's Linear Image Registration Tool; Jenkinson, Bannister, Brady, & Smith, 2002). This mask is an independent definition of white matter voxels in the FA map created from the DTI acquisition.

We used probabilistic tractography to define tracts connecting anterior frontal and posterior parietal cortices within each hemisphere. The cortical regions were defined from the Harvard-Oxford cortical atlas (Desikan et al., 2006). The superior lateral occipital complex was used as the posterior parietal region of interest (ROI) and lateral frontal pole ($X > |14|$) as the lateral prefrontal cortex ROI. Voxel-wise estimates of the fiber orientation distribution, including the modeling of up to two fibers per voxel, were calculated using Bedpostx (Behrens, Berg, Jbabdi, Rushworth, & Woolrich, 2007). Probabilistic fiber tracking was performed for each participant using the following settings: 5000 samples per voxel, maximum 2000 steps, curvature threshold of 0.2, 0.5 mm step length.

Left and right lateral fronto-parietal tracts were computed from anterior to posterior and posterior to anterior. 'Start' and 'stop' masks required tracts to pass through the two relevant cortical regions. Further, exclusion masks were used to restrict probabilistic streamlines to our *a priori* tracts. The exclusion mask for the fronto-parietal tracts prevented fibers that passed through the mid-sagittal plane, thalamus, basal ganglia, cingulum or insula from being included in our tract. All tractography was conducted in each participant's native DTI space, with masks transformed from standard space using FNIRT (FMRIB's Nonlinear Image Registration Tool, Andersson, Jenkinson, & Smith, 2007a, 2007b).

Upon completion of tractography for each participant, tract images were thresholded to remove voxels through which fewer than 5% of the total number of generated tracts passed. Anterior-to-posterior and posterior-to-anterior tracts were added together and binarized. Individual tract images for all participants were then overlaid on one another in standard space (Figure 3.1d).

These tract ROIs were transformed into subject space (using the non-linear warping described above) and white matter integrity within each tract was defined as the average of every voxel in the FA map that fell both inside the tract ROI and the subject's white matter mask ($WMI_{l\text{-}FPT}$). Whole brain WMI (WMI_{global}) was calculated for each subject as the average of every voxel in the FA map that fell within the subject's white matter mask.

Pairwise Regression Analyses with Age

The first step in our statistical analyses was to verify that our measures of fluid reasoning, processing speed and white matter integrity were increasing with age in our cohort. We fit data to a Von Bertalanffy exponential growth model of the form $y = \beta_1 + \beta_2 e^{\frac{age}{\beta_3}}$ separately for each of our dependent variables (FR, PS, WMI_{global}, right $WMI_{l\text{-}FPT}$ and left $WMI_{l\text{-}FPT}$). Regression analyses with age were performed in Stata 11 (StataCorp, 2009).

Structural Equation Modeling Analysis

Our goal in this study was to investigate the network of relations among fluid reasoning, processing speed, and white matter integrity. All SEM analyses were carried out using SEM in Mplus v6 (Muthen & Muthen, 1998). In our model, fluid reasoning was regressed on processing speed and both FR and PS were regressed on WMI. A Wald test was performed to assess the significance of removing the regression parameter from white matter on fluid reasoning. This model tests the hypothesis that higher white matter integrity leads to better cognitive processing speed leads which in turn leads to increased levels of fluid reasoning. This model was fit for each of the white matter ROIS separately.

3.3 Results

We replicated previous findings that cognitive processing speed, fluid reasoning and white matter integrity in all three white matter ROIs are increasing with age (Figure 3.2). Age predicts 74% of the variance in cognitive speed ($p < 0.001$, Figure 3.2A), and 62% of the variance in fluid reasoning ability ($p < 0.001$, Figure 3.2B). Similarly, age predicts 47% and 37% of the variance in FA in the right and left l-FPT ($p < 0.001$ for both, Figure 3.2C), and 42% of the variance in whole brain FA ($p < 0.001$, not shown). We also replicated previous findings that our neuropsychological tests of

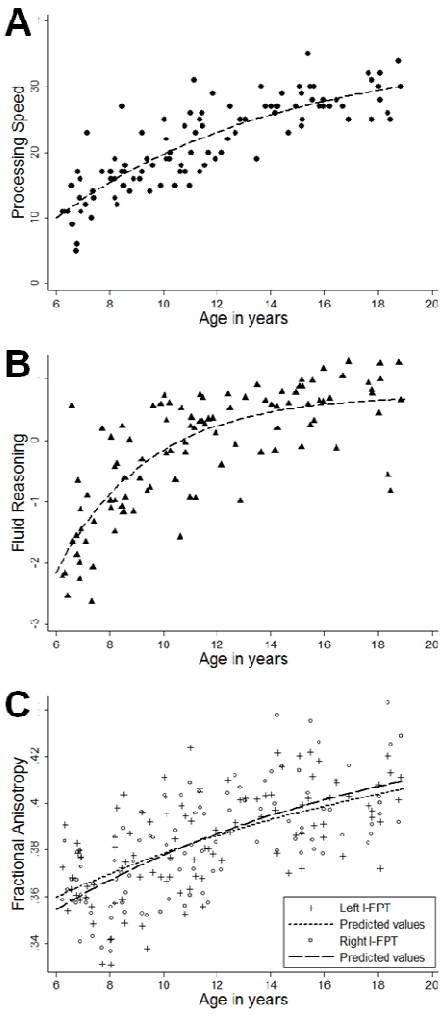

Figure 3.2: Development of processing speed (A), fluid reasoning (B) and white matter integrity (as indexed by fractional anisotropy, C) in left and right lateral fronto-parietal tracts.

fluid reasoning contribute strongly and equally to one latent variable. Factor scores are detailed in Table 3 1.

We hypothesized that the effect of white matter integrity on fluid reasoning was mediated by processing speed. We tested this hypothesis in three regions of interest: left and right lateral-frontoparietal tracts and whole brain white matter. Statistical fit indices for the mediation model for all three ROIs are reported in Table 3.1. For all three ROIs a Wald test of the regression from WMI to FR indicated that the parameter was not reliably different from zero ($P > 0.2$ for all ROIs) and thus its removal did not significantly affect the overall model fit. The most parsimonious model therefore is one in which FR is regressed on PS and PS on WMI with no direct link between FR and WMI (Figure 3.3). We conclude that the effect of white matter development on fluid reasoning is mediated by cognitive processing speed.

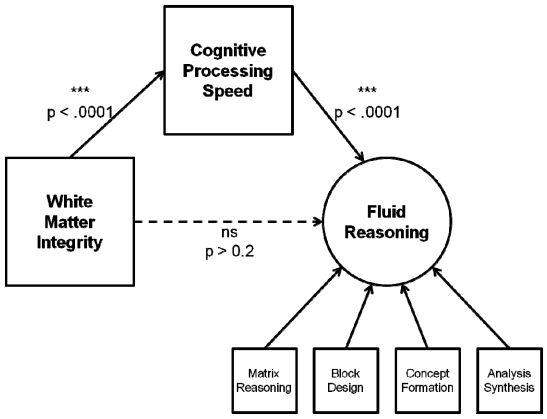

Figure 3.3: Structural equation model for the mediation of the effect of white matter integrity (as indexed by fractional anisotropy) on fluid reasoning by cognitive speed of processing. Models are explained in detail in Table 3.1 howeve the pattern is the same for all white matter regions of interest. The relationship between FR and WMI is mediated by cognitive processing speed.

3.4 Discussion

In this paper, we investigated the role of white matter integrity, as measured by FA, in both left and right l-FPT and the whole brain, in the relationship between fluid reasoning and processing speed. Our analyses indicate that the structure of the relations among processing speed, fluid reasoning, and global FA are best captured as unidirectional, with global FA predicting processing speed, and processing speed in turn predicting fluid reasoning. From these findings, the concurrent network of cognitive constructs and structural measures represents a chain in which white matter structural specialization is the leading indicator bringing about increases in processing speed, which, in turn lead to increases in fluid reasoning ability.

The inclusion of age is warranted in any developmental study, though the specification of its influence is not always straightforward. We showed that all our measures were significantly increasing with age but this does not elucidate the biological mechanisms which underlie the relationships. Practically speaking, age is a variable that summarizes changes in multiple factors that unfold together over time, whether these factors are interrelated or not. Age is therefore not really an explanatory variable, in that it does not provide mechanistic insights, as its inclusion in the modeling may imply. Here, we modeled multiple variables that all increase with age, and sought to understand how they relate to one another.

For this study we investigated two tracts of interest for which we hypothesized a relationship between WMI and FR, as well as a global measure of WMI from the whole brain. The global

Table 3.1: Standardized Estimates for the Mediation Model

Parameter	Estimate (SE)	Est/SE	P-value
Whole brain white matter			
Factor Loadings (FR)			
Matrix reasoning	.863 (.032)	26.72	< .0001
Block design	.868 (.033)	26.37	< .0001
Concept formation	.817 (.049)	16.63	< .0001
Analysis synthesis	.821 (.039)	20.96	< .0001
Regression Coefficients			
PS → FR	.750 (.066)	11.30	< .0001
Whole brain FA → PS	.577 (.066)	8.79	< .0001
Whole brain FA → FR	.092 (.082)	1.13	.259
Model fit			
CFI: 0.940; TFI: 0.887			
Right lateral fronto-parietal tract			
Factor Loadings (FR)			
Matrix reasoning	.864 (.032)	26.76	< .0001
Block design	.869 (.033)	26.44	< .0001
Concept formation	.814 (.050)	16.43	< .0001
Analysis synthesis	.820 (.039)	20.86	< .0001
Regression Coefficients			
PS → FR	.784 (.065)	12.04	< .0001
Right l-FPT FA → PS	.585 (.065)	9.04	< .0001
Right l-FPT FA → FR	.034 (.083)	0.41	.685
Model fit			
CFI: 0.940; TFI: 0.887			
Left lateral fronto-parietal tract			
Factor Loadings (FR)			
Matrix reasoning	.862 (.033)	26.53	< .0001
Block design	.871 (.033)	26.62	< .0001
Concept formation	.813 (.050)	16.28	< .0001
Analysis synthesis	.821 (.039)	20.89	< .0001
Regression Coefficients			
PS → FR	.757 (.061)	12.49	< .0001
Left l-FPT FA → PS	.515 (.072)	7.12	< .0001
Left l-FPT FA → FR	.092 (.039)	1.19	.235
Model fit			
CFI: 0.940; TFI: 0.887			

Note: FR = fluid reasoning; PS = processing speed; FA = fractional anisotropy

measure provides a more complete picture of the age-related changes in brain structure that support the development of processing speed and fluid reasoning, both of which rely on distributed brain networks. We did not find differences the pattern of our results between the tracts and our whole brain measure of WMI and thus conclude that the mediation of the relationship between WMI and FR by processing speed is an attribute of the whole brain, rather than specific regions of white matter. However, future research may indicate that particular regions, probably smaller in size than the whole l-FPT, play a more important role in processing speed and fluid reasoning than others..

The specific directions of relationships among the variables used in our models indicated that white matter is related to a network of cognitive variables, and this can reasonably be questioned. Neural structural development may be in part a consequence of increased activity in nerve fibers (Barres & Raff, 1993). The view that enhanced tract development precedes cognitive change may be an oversimplification. In fact, recent studies have shown that reasoning (Mackey, Whitaker, & Bunge, *in press*) can change white matter integrity in adults. Future studies of longitudinal data will be required to tease apart the reciprocal relationships between brain structure, brain function and cognition.

3.5 Conclusion

In sum, the present study contributes to our understanding of how structural brain changes support cognitive changes over development. Our modeling indicates that the strong relationship between white matter and fluid reasoning, reported both here and elsewhere (Chiang et al., 2009), is accounted for by improved speed of cognitive processing. Increased white matter coherence, caused both myelination and reorganization of white matter fibers, leads to more rapid transmission of information between brain regions. This increased speed of neuronal transmission results in faster processing at the level of brain networks, resulting in increased cognitive speed, which in turn makes possible the coordinated brain activity that is needed for the highest levels of human cognition.

Chapter 4: Global differences in the white matter of grapheme-color synesthetes correlate with the vividness of visual imagery

Author contribution statement

Bryan Alvarez: Designed the study, collected MRI data and wrote the manuscript
Kirstie Whitaker: Designed and conducted data analyses and wrote the manuscript
XJ Kang: Collected MRI data
Timothy Herron: Collected MRI data
David Woods: Designed the study
Lynn Robertson: Designed the study

4.1 Introduction

John Locke described the blending of senses that characterizes synesthesia in "An Essay Concerning Human Understanding" several centuries ago (Locke, 1689). In the time since, synesthesia has come to encompass a growing number of experientially-defined phenomena in which one cognitive domain (e.g., sounds, graphemes, language, emotions, etc.,) triggers another domain automatically, consistently, and consciously. Grapheme-color synesthesia is one of the most closely studied and most common varieties, characterized by consistent and automatic experiences of color triggered when viewing or imagining graphemes (e.g., letters, numbers, etc). Behavioral and brain-based research have lead to a number of new understandings about synesthesia, although synesthesia is by definition a subjective experience and more work is needed to link discoveries about brain mechanisms of synesthetes to their own elusive subjective experiences. In this study we examined how the neuroanatomy, specifically the white matter microstructure, of grapheme-color synesthetes may differ from that of non-synesthetes in relation to a behavioral metric (visual mental imagery) that is uniquely different among synesthetes while being generalizable into the non-synesthetic population.

Early brain-based models of grapheme-color synesthesia focused on the involvement of relatively local cortical regions and networks; area V4 (eg: Brang, Hubbard, Coulson, Huang, & Ramachandran, 2010; Hubbard, Arman, Ramachandran, & Boynton, 2005) and the lingual gyrus (Paulesu et al., 1995; Rich et al., 2006) were proposed to be involved in the origin of synesthetic color experience. Likewise, a surfeit of neuroanatomical (Rouw & Scholte, 2007, 2010; Weiss & Fink, 2009) and neurophysiological (Aleman, Rutten, Sitskoorn, Dautzenberg, & Ramsey, 2001; Beeli, Esslen, & Jäncke, 2008; Esterman, Verstynen, Ivry, & Robertson, 2006; Jäncke & Langer, 2011; Muggleton, Tsakanikos, Walsh, & Ward, 2007; Neufeld et al., 2012; Nunn et al., 2002; Paulesu et al., 1995; Rothen, Nyffeler, von Wartburg, Müri, & Meier, 2010; Steven, Hansen, & Blakemore, 2006; Weiss, Zilles, & Fink, 2005; van Leeuwen, Petersson, & Hagoort, 2010) data suggest the role of parietal and frontal regions in the integration and binding of synesthetic phenomenology. Local regions likely do play a role in synesthetic neurophysiology, however a number of studies have failed to confirm the role of V4 in grapheme-color synesthesia (Hupé, Bordier, & Dojat, 2012; Rich et al., 2006; Rouw & Scholte, 2007) and a new pattern of has emerged supporting the involvement of highly distributed cortical areas in synesthetic representation relative to non-synesthetic controls that rely heavily on parieto-frontal regions, giving new meaning to the role of these networks (Dovern et al., 2012; Hupé et al., 2012; Hänggi, Wotruba, & Jäncke, 2011). Parietal lobe function has been linked with a multitude of

behaviors, and is best described as *association cortex*, receiving inputs from all regions of the brain (Hagmann et al., 2008). Seen in this context, is not surprising that synesthetes would demonstrate differences in this region of cortex, since synesthetes are blending together information from multiple cognitive domains above and beyond the norm.

For disparate brain regions to communicate efficiently action potentials must be transmitted relatively long distances along myelinated axons, which make up the brain's "white matter". White matter microstructure can be investigated *in vivo* using diffusion tensor imaging (DTI). As water diffuses, it follows the path of least resistance, and therefore preferentially moves along axons, particularly for myelinated axons in a coherent fiber tract (Beaulieu, 2002; Assaf & Pasternak, 2008). Diffusion-weighted MRI is sensitive to the direction of water movement and, after fitting this movement to a tensor model, several measures are commonly extracted. Fractional anisotropy (FA), a scaled ratio of the propensity of water to diffuse along the axon (parallel diffusivity, λ_1) versus across it (perpendicular diffusivity, λ_{23}), is a measure of white matter coherence (Basser, 1995; Pierpaoli & Basser, 1996). Mean diffusivity (MD) is the average of diffusion in all three orthogonal directions. We hypothesized that synesthetes would demonstrate globally distributed differences in FA due to differences in their underlying white matter microstructure.

If grapheme-color synesthesia is an indicator (which may or may not generalize across the synesthetic continuum) of a highly distributed, systemically different neural network relative to non-synesthetes, it would be expected that this population would show differences beyond their specific synesthetic experiences. Indeed, grapheme-color synesthetes show widely distributed increases in neural activity (Barnett et al., 2008) and increased cross-modal interactions (vision and audition) in response to stimuli that do not induce synesthetic color (Brang, Williams, & Ramachandran, 2012). Grapheme-color synesthetes have shown increased excitability in the primary visual cortex (Tehrune, Tai, Cowey, Popescu, Cohen Kadosh, 2011), more accurate color discrimination (Yaro & Ward, 2007), better memory (Smilek, Dixon, Cudahy, & Merikle, 2002; Yaro & Ward, 2007), stronger visual imagery (Barnett & Newell, 2008) and heightened creativity (Mulvenna, Hubbard, Ramachandran, & Pollick, 2003; Ward, Thompson-Lake, Ely, & Kaminski, 2008) relative to matched controls. With the possible exception of color discrimination, these factors do not rely specifically on color-selective area V4 or any other single neural locus implied specifically in synesthetic experience.

If specific and unimodal forms of synesthesia such as grapheme-color reflect a broadly distributed pattern of neural activity and anatomy, one might expect to find a correlative behavioral metric that is equally broad, while also being unique in some way to synesthesia. Rouw and Scholte (2007) offer a piece of critical evidence, showing that grapheme-color synesthetic experience can be correlated with differences in white matter integrity. In this study we pursued this finding further, asking whether white matter integrity correlates with a measure of phenomenology common to most humans, but perhaps unique within the synesthetic population: the vividness of visual imagery.

Visual imagery is the ability to "see in the mind's eye" when there are no external stimuli present. There are many ways that synesthetic experience is likened to visual mental representations. Grapheme-color synesthesia can be triggered simply by imagining a grapheme

when a physical stimulus is not present (Elias, Saucier, Hardie, & Sarty, 2003; Jansari, Spiller, & Redfern, 2006; Spiller & Jansari, 2008), and this is likely the norm rather than the exception. Connections between synesthesia and imagery were proposed early on by Ramachandran and Hubbard (2001) and have been substantiated in synesthetic populations (Barnett & Newell, 2008; Price, 2009). Barnett and Newell (2008) showed that a generalized population of synesthetes showed more vivid mental imagery than controls.

Here, we address the degree to which differences in white matter structure in grapheme-color synesthesia are globally distributed and correlate with a behavioral measure that is not unique to synesthesia *per se*: visual imagery (Marks, 1973). We aim to replicate previous studies, showing that synesthetes have more vivid visual imagery (VVI) than closely matched non-synesthete controls. We then test whether synesthetes show differences in white matter integrity compared with well matched, yoked controls. Finally, we investigate the relationship between VVI and white matter integrity in our synesthetic and control populations to see how a cognitively distributed (Mechelli, Price, Friston, & Ishai, 2004) behavior such as mental imagery correlates with global differences in neuroanatomy.

4.2 Results

Behavioral differences in visual imagery

All participants completed the Vividness of Visual Imagery Questionnaire (Marks, 1973) by rating a series of questions about their own imagery. All scores were scaled between 0 and 1, where a score of 1 represents imagery as vivid as perception, and a score of 0 represents little to no mental imagery. As illustrated in Figure 4.1, we replicated previous findings that grapheme-color synesthetes have more vivid visual imagery than non-synesthete controls (student's $t(38) = 2.53$, $p < 0.05$, two-tailed).

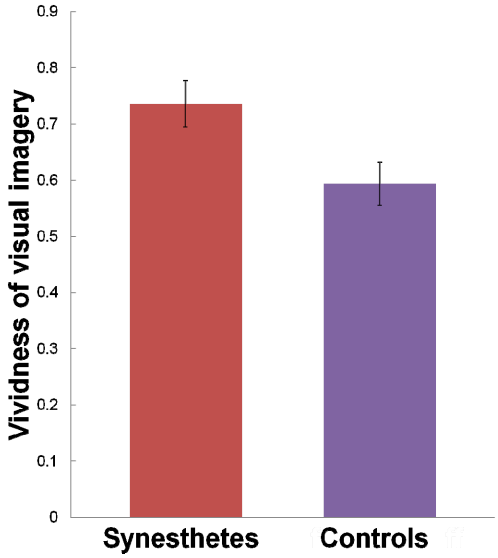

Figure 4.1: Differences in vivid visual imagery (VVI) between synesthetes and control participants (error bars are standard error). Synesthetes had significantly higher VVI scores than non-synesthete controls

Group differences in white matter integrity

We investigated voxel-based measures of white matter integrity throughout the brain for all participants using diffusion tensor imaging. We conducted student's t tests to look for differences in mean value for four measures of white matter microstructure (FA, λ_1, λ_{23} and MD). We found significant differences in FA and λ_{23} in widespread areas throughout the brain (Figure 4.2) corresponding to synesthetes having lower FA and higher λ_{23} than non-synesthete controls. There were no differences between groups in λ_1 or MD. Table 4.1 lists the percentage of each white matter region of interest within the Johns Hopkins University (JHU) White Matter Label Atlas (Mori, 2005) that

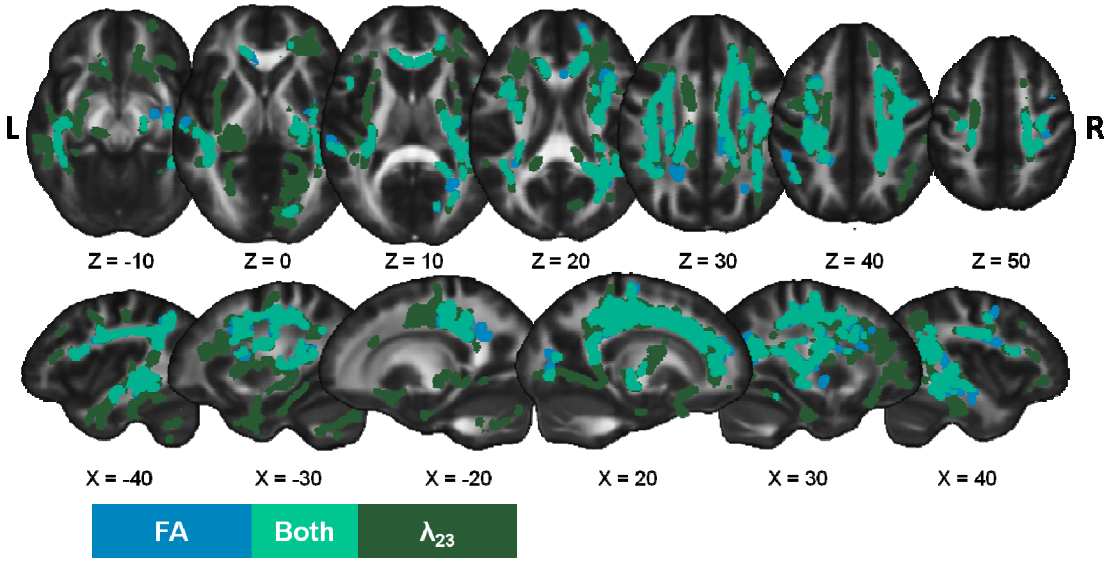

Figure 4.2: Whole brain results of TBSS analysis showing significant differences between synesthetes and non-synesthete controls. Synesthetes had significantly lower FA (blue) and higher L23 (green) in many regions through the brain. All analyses were performed on the white matter skeleton; results were filled for easier visualization.

shows significant differences between synesthetes and controls.

To better characterize the anatomy of the white matter regions that were different between synesthetes and controls we investigated the mode of anisotropy, a recently developed tensor index (Ennis & Kindlmann, 2006) that can be used to identify regions of crossing fibers. We extracted the average mode from every voxel on the white matter skeleton that showed significant differences between synesthetes and controls (Figure 4.3). Synesthetes had significantly lower median mode (*Mann-Whitney* $U = 2.01 \times 10^{11}$, $df = 129816$, $P < 1 \times 10^{-100}$) when compared to non-synesthete controls.

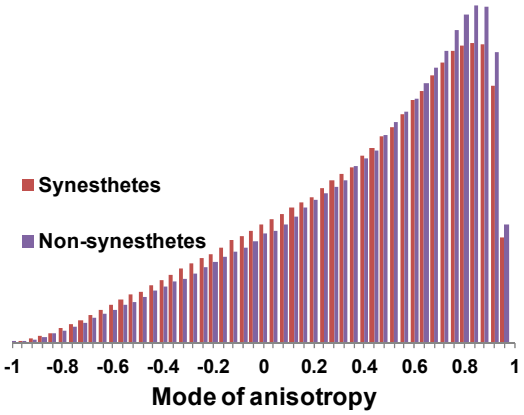

Figure 4.3: Distributions of mode values within voxels showing differences in white matter integrity (FA and L23) between controls and synesthetes. Synesthetes have a significantly lower median mode which is indicative of less coherent white matter tracts in these regions.

Correlations between visual imagery and white matter

We next conducted a Pearson's correlation between VVI scores and DTI measures of white matter integrity in order to investigate the individual differences in brain and behavior. As shown in Figure 4.4, we found a strong negative correlation between VVI and FA throughout the brain for all participants. This was accompanied by a strong positive correlation with λ_{23}. The percentage of each white matter region of

White Matter Labels	Voxels in white matter skeleton	Group differences (% of skeleton)		
		FA	L23	Both
Body of corpus callosum	3217	19.2	31.5	17.6
Splenium of corpus callosum	2648	10.3	25.1	8.1
Genu of corpus callosum	1789	11.6	43.1	6.5
Fornix	786	31.6	38.2	29.9
L anterior corona radiata	1800	7.2	8.3	7.2
R anterior corona radiata	1721	25.6	40.7	24.5
L superior corona radiata	1354	31.9	56.9	28.7
R superior corona radiata	1362	24.6	67.8	21.1
L posterior corona radiata	748	23.0	49.2	16.6
R posterior corona radiata	846	20.2	51.9	17.1
L superior longitudinal fasciculus	1450	16.6	54.4	12.6
R superior longitudinal fasciculus	1514	20.4	63.5	15.2
L superior fronto-occipital fasciculus	100	28.0	28.0	28.0
R superior fronto-occipital fasciculus	113	0.0	0.0	0.0
L uncinate fasciculus	65	0.0	0.0	0.0
R uncinate fasciculus	69	39.1	39.1	39.1
L posterior thalamic radiation	1103	9.3	16.4	8.9
R posterior thalamic radiation	1141	15.2	35.4	11.7
L cingulum	661	14.7	21.9	13.3
R cingulum	716	13.5	23.6	11.5
L sagittal stratum	489	33.5	66.7	32.5
R sagittal stratum	576	20.3	42.2	10.9
L internal capsule	2367	7.5	14.2	5.9
R internal capsule	2484	14.7	36.3	12.0
L external capsule	1443	31.3	31.8	30.8
R external capsule	1302	18.3	27.7	12.7
Cerebellum	4273	5.7	5.7	5.7
Brainstem	2490	18.1	19.2	18.0
Not classified	157763	11.5	21.6	20.9

Table 4.1: Regions of the JHU White Matter Label Atlas that show significant differences between synesthetes and non-synesthete control participants. The number of voxels in the white matter skeleton which fall in each label is listed along with the percentage of these voxels which show significant differences in FA, L23 and both measures.

interest from the JHU atlas (Mori, 2005) that showed significant correlations between FA, λ_{23}, or both, and VVI is tabulated in Table 4.2.

Given the group differences in both brain (Figure 4.2) and behavior (Figure 4.1), we chose to investigate correlations in the two groups separately. We saw similar results in synesthetes (negative correlation with FA, positive correlation with λ_{23}, Figure 4.5 and Table 4.2) although the regions which demonstrated significant correlations were more restricted to association cortex. We found no significant results in non-synesthete controls. In order to visualize the correlation, we extracted average FA from every voxel which showed a significant correlation with either FA or λ_{23} when synesthetes were examined alone (Figure 4.5) for both synesthetes and controls. Figure 4.5B illustrates the negative correlation between FA and VVI for synesthetes (for which no statistics are performed as it is defined by the voxels we averaged the data over). In comparison, average FA from the same voxels in control participants showed no correlation (r^2 = 0.004, P = 0.79, Figure 4.5B).

Since it is difficult to interpret the lack of significant results in the control group, we tested the difference in correlations for synesthetes and non-synesthete controls. We found several regions for which the positive correlation between VVI and λ_{23} was stronger in synesthetes than controls: bilateral posterior corona radiata, left superior corona radiata, and the body of the corpus callosum (Figure 4.5). There were no regions that showed a significantly larger correlation in synesthetes than controls for FA.

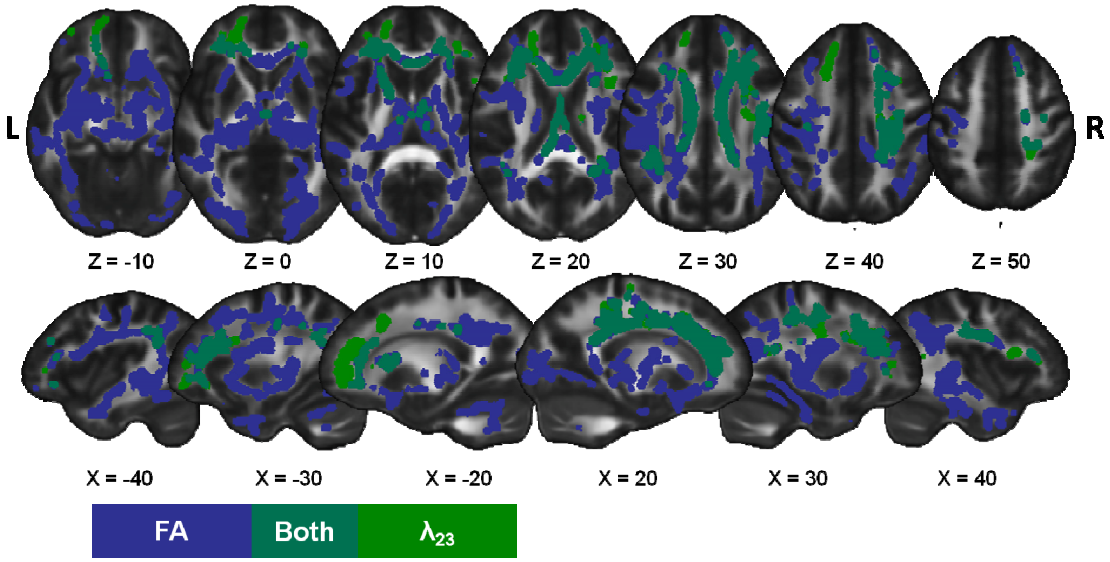

Figure 4.4: Whole brain results of TBSS analysis showing significant correlations between VVI and FA (negative, blue) or λ23 (positive, green) in all participants. All analyses were performed on the white matter skeleton; results were filled for easier visualization.

4.3 Discussion

This study is the first to provide evidence that grapheme-color synesthetes show globally distributed differences in white matter integrity that correlate with the vividness of visual imagery. Synesthetes show significantly lower FA throughout white matter and statistically higher scores on the test of the vividness of visual imagery. These lower global FA and higher average VVI scores are corroborated by a significant negative correlation unique to synesthetes between FA and VVI: synesthetes with the lowest FA also have the most vivid visual imagery.

Neuroanatomical differences in grapheme-color synesthetes are increasingly common (Rouw and Scholte, 2007; Rouw and Scholte 2010; Weiss and Fink, 2008; Jäncke et al., 2009; Hupé et al., 2011; Hänggi et al., 2012). Moreover, newly reported differences in the structural integrity of the grapheme-color synesthete brain appear to be globally distributed (Hupé et al., 2011) in hyperconnectivity (Hänggi et al., 2012) and functional resting-state connectivity (Dovern et al., 2012), regardless of the unresolved inconsistencies in the direction of difference.

Our study is the first to investigate the mode of anisotropy in synesthetes. We show that the regions with lower FA and higher λ_{23} in synesthetes, when compared to controls, also have lower mode values. Recent work by Douaud and colleagues (2011) has shown *higher* FA in the centrum semiovale in older adults with mild cognitive impairment (MCI) when compared to age-matched controls. They also report higher mode values in the MCI group in this region, where two fiber tracts cross. Their study shows that as one tract deteriorates, the mode and FA increase because white matter becomes more coherent in these regions.

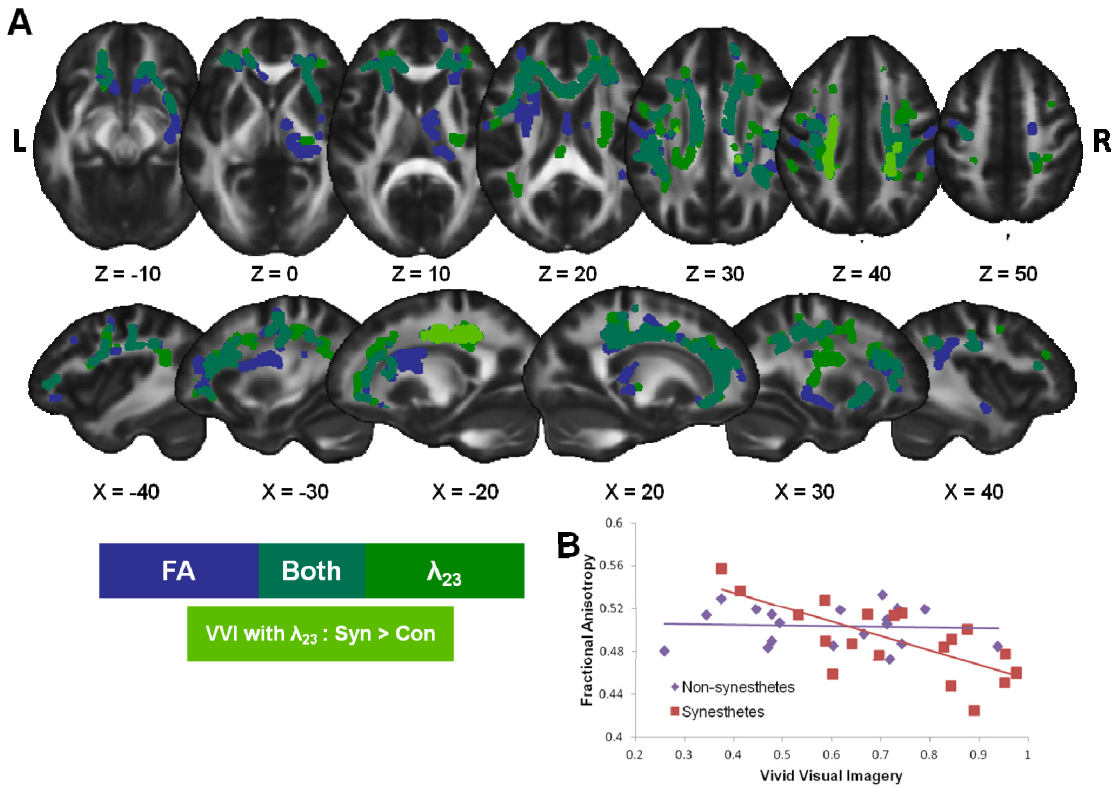

Figure 4.5: A) Whole brain results of TBSS analysis showing significant correlations between VVI and FA (negative, blue) or λ_{23} (positive, green) in synesthetes alone. Bright green tracts in the left and right corona radiata are those voxels for which the correlation in synesthetes is significantly larger than the correlation in non-synesthete controls. All analyses were performed on the white matter skeleton; results were filled for easier visualization. B) The correlation of average FA in all voxels of the white matter skeleton that show a significant relationship between FA and/or λ_{23} for synesthetes is plotted for visualization purposes only. Synesthetes and non-synesthete controls are plotted separately. No statistics are performed on these data.

This leads us to interpret the differences between synesthetes and non-synesthete controls as due to less coherent white matter structure throughout the brain rather than a difference in myelination. The axons in the synesthetes' brains are going in different directions, and connecting more disparate regions of cortex.

The results presented in the current study further validate findings showing widely distributed differences in white matter integrity throughout the brain. Grapheme-color synesthetes have shown enhanced memory (Rothen & Meier, 2010; Smilek et al., 2002; Yaro & Ward, 2007), more vivid visual imagery (Barnett & Newell, 2008), heightened creativity (Mulvenna et al., 2003; Ward et al., 2008), increased cross-modal interactions (vision and audition) in response to stimuli that do not induce synesthetic color (Brang et al., 2012), and increased visual activation

White Matter Labels	Correlation with VVI					
	All participants (% of skeleton)			Synesthetes only (% of skeleton)		
	FA	L23	Both	FA	L23	Both
Body of corpus callosum	22.8	57.6	1.5	15.5	46.3	8.6
Splenium of corpus callosum	20.3	10.3	0.2	3.0	2.3	1.4
Genu of corpus callosum	29.5	30.6	0.7	9.7	20.0	0.8
Fornix	56.2	9.3	0.9	19.7	0.0	0.0
L anterior corona radiata	22.6	33.7	7.1	22.2	41.9	9.9
R anterior corona radiata	27.7	37.9	1.9	15.8	52.5	4.3
L superior corona radiata	30.5	2.9	0.4	24.8	26.1	8.6
R superior corona radiata	30.0	28.0	8.6	24.1	38.0	21.9
L posterior corona radiata	34.5	0.4	0.0	27.8	27.8	27.8
R posterior corona radiata	14.2	14.5	0.6	8.5	26.8	4.3
L superior longitudinal fasciculus	47.1	6.8	0.2	14.3	26.3	6.1
R superior longitudinal fasciculus	24.4	26.0	4.3	11.5	19.4	3.3
L superior fronto-occipital fasciculus	12.0	0.0	0.0	0.0	0.0	0.0
R superior fronto-occipital fasciculus	0.0	0.0	0.0	70.8	0.9	0.0
L uncinate fasciculus	87.7	0.0	0.0	26.2	52.3	0.0
R uncinate fasciculus	55.1	0.0	0.0	0.0	0.0	0.0
L posterior thalamic radiation	33.3	0.0	0.0	0.3	0.3	0.3
R posterior thalamic radiation	28.1	4.8	0.3	0.0	0.0	0.0
L cingulum	6.2	7.9	1.2	1.5	2.9	1.5
R cingulum	24.7	5.0	0.3	0.4	4.5	0.3
L sagittal stratum	44.2	0.0	0.0	0.0	0.0	0.0
R sagittal stratum	43.2	0.0	0.0	2.3	0.0	0.0
L internal capsule	19.3	6.6	0.2	3.6	0.3	0.0
R internal capsule	45.0	0.0	0.0	5.6	5.0	5.0
L external capsule	42.3	0.0	0.0	1.6	0.1	0.1
R external capsule	47.1	0.0	0.0	15.1	18.0	2.2
Cerebellum	20.4	0.0	0.0	0.0	0.0	0.0
Brainstem	39.9	0.0	0.0	0.0	0.0	0.0
Not classified	27.8	34.6	8.8	8.5	11.0	10.0

Table 4.2: Regions of the JHU White Matter Label Atlas that show significant correlations between VVI and FA, λ_{23} or both measures of white matter integrity. The number of voxels in the white matter skeleton that fall in each label is as listed in Table 4.1 and the percentage of these voxels that show significant correlations with FA, λ_{23} and both measures are shown for the analysis of all participants (Figure 4.4) and synesthetes alone (Figure 4.5).

throughout the ventral visual stream in response to stimuli that do not trigger any specific synesthetic experience (Barnett et al., 2008)

It is of particular note that the regions in which we see the strongest correlation between white matter integrity and VVI (Figure 4.5) are tracts near association cortex, the axons from which, by definition, project to and from many different cortical targets. Parietal cortex in particular is ubiquitous to both synesthetic neuroanatomical findings and associative processing in general due to its role as a hub of cortical and subcortical interconnectivity in the human brain (Hagmann et al., 2008). It is possible that the phenomenology of grapheme-color synesthesia represents differences in parietal function (Specht & Laeng, 2011). Given the widespread connectivity of the parietal lobe, which is thought to play a role in binding synesthetic color in synesthetes (Esterman et al., 2006; Robertson, 2003), and the fact that grapheme-color synesthetes show some advantage beyond their synesthetic modalities alone, we looked beyond synesthetic experience to examine relationships between behavioral and neuroanatomical differences in this population.

Grapheme-color synesthetes in the present study have more vivid visual imagery than matched controls, replicating a similar result reported by Barnett and Newell (2008). As seen in Figure 4.5, synesthetes show significant correlations with FA and λ_{23} and visual imagery through

fronto-parietal networks, but not within early visual regions. Given that all synesthetic subjects experienced colored graphemes, and that 17 of the 20 experienced colors in their mind's eye only ("associator" synesthetes), it is likely that these synesthetes as a group have similar visual cortices. However, as visual imagery becomes more vivid for synesthetes, white matter integrity in fronto-parietal networks decreases, becoming less like the non-synesthete control group. Individual differences that are not present in white matter near early visual cortex become apparent in tracts connecting association cortices.

The negative correlation with WMI and VVI may also represent a different strategy for grapheme-color synesthetes. Synesthetes with vivid imagery/lower FA may rely on increasingly visual-based forms of imagery, whereas synesthetes that follow a pattern more similar to controls may show a more typical memory-based strategy of imagery. Further studies are needed to investigate the role of white matter and visual imagery in strategy differences for grapheme-color synesthetes.

4.4 Conclusion

Grapheme-color synesthetes in this study show significant decreases in white matter integrity throughout much of brain, and more vivid self-reported visual imagery compared to a control group of non-synesthetes. Reported decreases in FA are likely due to a higher degree of crossing fibers in synesthetes. A significant negative correlation between FA and visual imagery, specific to the synesthete population, was found. Synesthetes with the lowest white matter integrity (FA) had the most vivid visual imagery.

4.5 Methods

Participants
Twenty grapheme-color synesthetes and twenty non-synesthete controls participated in this study. All participants had normal or corrected to normal vision, no reported history of neurological or psychiatric disorder, and gave signed informed consent before entering the study as approved by the institutional review board of Veterans Affairs. Synesthesia was verified with the Online Synesthesia Battery (Eagleman, Kagan, Nelson, Sagaram, & Sarma, 2007) and only those who showed consistent and conscious experience of grapheme-color synesthesia were considered eligible as synesthetic subjects, although several grapheme-color synesthetes also reported other forms of synesthesia. Non-synesthete controls also participated in the Synesthesia Battery to assure that they experienced no forms of synesthesia. All controls were additionally questioned in person about their conscious experience of several other synesthetic varieties and only controls that experienced no forms of synesthesia were included in the study. Participants were paid $12 per hour for their involvement in the study.

Synesthetes and controls were meticulously matched for sex, age, handedness, and years of education, all of which can influence neuroanatomy. All participants were between the ages of 19 and 35 (M = 25.8, SD = 4.1, 34 female) and between 14 and 24 years of education (M = 18.1, SD = 2.3). Each control was yoked to a synesthete meaning that each control was the same sex and handedness and in most cases the exact or nearly the same age and years of education.

Visual Imagery Assessment

All subjects completed the Vividness of Visual Imagery Questionnaire (Marks, 1973). This questionnaire consists of 4 sets of 4 questions (16 in total) each asking the participant to imagine specific scenarios relating to a topic first with their eyes open and then to answer all 16 questions again with their eyes closed. The subjective report of the vividness of visual imagery is rated by the participant on a 5 point Likert scale where a score of 1 indicates the imagined image is "perfectly clear and as vivid as normal vision" and a score of 5 indicates "no image at all, you only 'know' that you are thinking of an object". These scores were scaled to range between 0 and 1, with 1 representing the "best" visual imagery and 0 representing very poor visual imagery to allow the correlation analyses presented in the results section to be more easily understood. Since there was no significant difference between the scores for eyes open or eyes closed, the rest of our analyses focused on the average of each participant's scores.

Diffusion Tensor Imaging Data Acquisition and Preprocessing

Brain imaging data was collected at the Veterans Affairs Clinic in Martinez, California on a 1.5 T Eclipse Phillips MR scanner using a 4-channel head coil with a maximum gradient strength of 40mT/m. Each participant underwent four sets of cardiac-gated DTI scans using echo-planar imaging (EPI; TR depends on the participant's heart rate; TE = 115.6 ms; 3 mm^3 isotropic voxels). Two non-diffusion-weighted image and 6 diffusion-weighted directions were acquired per scan, with a b-value of 1000 s/mm^2. A T1-weighted image was also acquired in each participant for image registration (TR = 15ms; TE = 4.47 ms; voxel size 1.3 x 0.94 x 0.94 mm^3).

Analyses were performed using tools from FDT (for Functional MRI of the Brain (FMRIB) Diffusion Toolbox, part of FSL 4.1, Smith, 2002; Woolrich et al., 2009). Brain volumes were skull stripped using the Brain Extraction Tool (Smith, 2002) and a 12 parameter affine registration to the non-diffusion weighted volume was applied to correct for head motion and eddy current distortions introduced by the gradient coils. A diffusion tensor model was fitted to the data in a voxelwise fashion to generate whole-brain maps of the three orthogonal eigenvectors and eigenvalues, mean diffusivity (MD), and fractional anisotropy (FA). We shall refer to the largest eigenvalue (λ_1) as *parallel diffusivity* and the average of the two remaining eigenvalues as *perpendicular diffusivity* (λ_{23}).

A white matter mask was created from each participant's high resolution T1-weighted scan, after brain extraction, using FAST (FMRIB's Automated Segmentation Tool; (Zhang, Brady, & Smith, 2001), which segments the brain into grey matter, white matter, and cerebral spinal fluid. This mask was transformed into the participant's DTI space by applying the inverse of the affine registration of the non-diffusion weighted volume to the high resolution image. Both the registration and calculations of the inverse transform used FLIRT (FMRIB's Linear Image Registration Tool; Jenkinson, Bannister, Brady, & Smith, 2002). This mask is an independent definition of white matter voxels in the FA map created from the DTI acquisition.

Finally, each of the participants' FA maps were aligned into standard space using FNIRT (FMRIB'S Nonlinear Image Registration Tool; Andersson, Jenkinson, & Smith, 2007a, 2007b). By applying the same transform, mean diffusivity, parallel and perpendicular diffusivity, and the white matter mask were also transformed into standard space.

DTI Analyses: Tract-based Spatial Statistics

We performed voxel-wise statistical analysis using TBSS (Tract-Based Spatial Statistics, Smith et al., 2006). After FA maps were aligned to standard space, the mean FA image was generated and thinned to produce a mean FA skeleton that represented the centers of all tracts common to the group. Each subject's aligned FA, λ_1, λ_{23}, and MD data were then projected onto this skeleton by finding the nearest maximum FA value for the individual. This projection step aims to remove the effect of cross-subject spatial variability that remains after the non-linear registration. Voxel-wise cross-subject permutation-based nonparametric statistics were performed using Randomise (Nichols & Holmes, 2002) with 5000 permutations and threshold-free cluster enhancement to correct for multiple comparisons at $P < .05$ (Smith & Nichols, 2009).

We conducted three specific statistical tests on each of the measures of white matter integrity (FA, λ_1, λ_{23} and MD) in turn. The first, a student's T-test on the difference of means between synesthestes and controls. Second, a Pearson's correlation between white matter integrity and average VVI for the whole group, and each group separately. Finally, we looked for regions in which the correlation between VVI and white matter integrity was significantly different for synesthetes and controls, controlling for differences in mean white matter measures.

To better characterize the anatomy of white matter showing an effect of training, we examined a recently developed tensor index used to identify regions of crossing fibers (Douaud et al., 2011): the mode of anisotropy (Ennis & Kindlmann, 2006). Regions with a positive mode have linear anisotropy, and are likely to be part of a highly directional tract. In contrast, regions with a low or negative mode can be described as having planar anisotropy, and are more likely to contain crossing fibers. We extracted mode of anisotropy values from voxels that were significantly different between synesthetes and non-synesthete controls. Specifically, we extracted values from every participant's mode map after it had been registered into standard space by following the non-linear warping described above. Histograms with a bin width of 0.04 were created using fslstats, an FSL tool (Smith et al., 2004). We used a Mann-Whitney *U*-test to compare the distributions of mode values within these results for synesthetes and non-synesthete controls.

Chapter 5: Experience-dependent plasticity in white matter microstructure: Reasoning training alters structural connectivity

Author contribution statement

Allyson Mackey: Designed the study, collected MRI data, designed and conducted data analyses and wrote the manuscript
Kirstie Whitaker: Designed and conducted data analyses and wrote the manuscript
Silvia Bunge: Designed the study and wrote the manuscript

5.1 Introduction

Advances in neuroimaging techniques have led to important progress in understanding how brain regions are structurally and functionally connected in the human brain. Much of this knowledge has been obtained from cross-sectional studies, which provide only a snapshot of an individual's brain at a single point in time. As a result, we have only just begun to understand how learning and experience shape brain connectivity. In this paper, we provide evidence for experience-dependent changes in white matter microstructure among young adults participating in intensive cognitive training.

White matter microstructure can be investigated *in vivo* using diffusion-weighted imaging (DWI). DWI relies on the biophysical principal that, as water diffuses, it follows the path of least resistance. Water diffusing in any given white matter voxel encounters axons (which contain dense cytoskeletons, are bounded by cellular membranes, and are surrounded by myelin) and glial cells. Research in animals has shown that water preferentially moves along axons rather than through the myelin sheath (for review see Beaulieu, 2002; Assaf & Pasternak, 2008). Activity-dependent increases in myelination could, therefore, reduce diffusion through the myelin sheath. However, changes in unmyelinated axons, and the number and/or size of glia, could also alter diffusion.

Diffusion tensor imaging (DTI) analysis fits a tensor to DWI to extract measures of axial diffusion (axial diffusion (AD or λ_1)), the preferential direction of water diffusion, and radial diffusion (RD or λ_{23}), the average of the two directions perpendicular to AD. AD has been related to diffusion along an axon, whereas RD is linked to diffusion through the myelin sheath (Beaulieu, 2002). Fractional anisotropy (FA) is a scaled ratio of AD to RD (Basser, 1995; Pierpaoli & Basser, 1996). High FA indicates strong directionality of water diffusion, i.e., high white matter coherence. Mean diffusivity (MD) is the average of diffusion parameters in all three orthogonal directions. Low MD reflects a high density of cells and/or extracellular material that impedes the diffusion of water through brain tissue. Because these diffusion measures (AD, RD, FA, and MD) have been shown to relate to different aspects of white matter composition (Song et al., 2002, 2003), some DTI studies of neuroplasticity have investigated the measures separately, though many have focused specifically on FA.

Neuroplasticity in humans has been studied through two main approaches. A first approach has been to compare experts to novices, with the assumption that any brain differences between the groups can be attributed to the extensive training experts have received over the course of their lives. This work has yielded mixed results in terms of the direction of observed differences in

DTI measures. For example, when comparing musicians to non-musicians, both increased and decreased FA in the corticospinal tract have been observed (Imfeld, Oechslin, Meyer, Loenneker, & Jancke, 2009). Additionally, when comparing fighter pilots – who demonstrate enhanced cognitive control relative to the general population – with controls, lower RD in white matter underlying parietal cortex and higher RD in white matter near medial frontal cortex were observed (Roberts, Anderson, & Husain, 2010). In such studies, it is not possible to disambiguate the effects of experience from an innate predisposition to pursue a particular type of training.

A second approach to studying neuroplasticity in humans involves direct experimental control over individuals' experience. To date, there have been very few published studies on training-related plasticity in white matter microstructure in healthy adults. One study showed that working memory training increased FA in left parietal and frontal white matter, as well as white matter under somatomotor cortices (Takeuchi et al., 2010). However, this study did not include a control group, so effects of maturation in the study's young participants cannot be ruled out. A second study showed that juggling training increased FA in white matter near right posterior parietal cortex, potentially related to enhanced use of visual areas important for detecting motion (Scholz, Klein, Behrens, & Johansen-Berg, 2009). A third study showed decreased FA in bilateral frontal lobes, and increased mean diffusivity (MD) in right parietal lobe and cerebellum following practice with a balancing task (Taubert et al., 2010). Finally, a fourth study showed that meditation training leads to increased FA in medial anterior corona radiata (Tang et al., 2010). Further analysis of this data set revealed that the majority of voxels exhibiting increased FA showed both decreased RD and AD (Tang, Lu, Fan, Yang, & Posner, 2012).

In the present study, we investigated white matter changes associated with intensive training on relational reasoning, the ability to compare and combine mental representations. The reasoning training paradigm consisted of a course aimed at improving scores on the Law School Admissions Test (LSAT). The LSAT has three parts: Logic Games, Logical Reasoning, and Reading Comprehension (for a sample test, see http://www.lsac.org/jd/pdfs/SamplePTJune.pdf). Both of the logic sections heavily tax relational reasoning. Because this exam plays an almost determinative role in law school acceptance, we reasoned that students would be highly motivated to prepare for it.

Numerous studies have implicated a bilateral fronto-parietal network in reasoning (see Krawczyk, 2012; Hampshire, Thompson, Duncan, & Owen, 2011; Prado, Chadha, & Booth, 2011 for review), several of which have suggested that rostrolateral prefrontal cortex (RLPFC) is specifically involved in relational integration (Hampshire et al., 2011; Wendelken & Bunge, 2010; Wendelken, Chung, & Bunge, 2011; Wendelken, O'Hare, Whitaker, Ferrer, & Bunge, 2011). Based on these findings, we predicted changes in white matter connecting frontal and parietal cortices both within and between hemispheres. We were specifically interested in changes in the trained group that were significantly greater than those measured for an age- and IQ-matched control group. In other words, we considered changes in the trained group that could not be accounted for by typical development in young adults over 3 months to be the strongest evidence for experience-dependent plasticity.

5.2 Methods

Participants

Twenty-five adults (14 females) took part in the training group, and twenty-five adults (14 females) took part in the age- and IQ-matched pre-law control group (Table 1). The training group was recruited through e-mail and classroom announcements to students in Blueprint Test Preparation courses. The control group was recruited through e-mails to pre-law organizations and online postings. Recruitment and experimental procedures were approved by the Committee for the Protection of Human Subjects at the University of California at Berkeley. Participants had no history of psychiatric or neurological disorder, and were fluent in English. Three participants in the trained group and two participants in the control group were left-handed.

Table 5.1: Demographic and behavioral measures for study participants. Means and standard deviations are reported. None of the measures differed significantly between groups ($P > .2$).

	Trained ***N* = 23**	**Control** ***N* = 22**
Age	21.39 (1.42)	21.44 (2.15)
WASI Matrix	29.75 (2.10)	29.37 (1.74)
WASI Vocabulary	66.33 (5.76)	67.10 (3.67)
Days between scans	89.17 (15.61)	90.91 (22.87)
Perceived Stress Time 1 Time 2	 21.67 (7.71) 21.16 (7.07)	 20.24 (7.32) 22.11 (9.13)
Hours of Sleep Time 1 Time 2	 7.50 (0.88) 7.33 (1.08)	 7.57 (0.96) 7.34 (1.14)

Two participants – one from each group – were excluded from the study because they exhibited dramatic changes in stress levels and amount of sleep from time 1 to time 2 (more than 3 SD from the mean of all participants). Additionally, two participants from the control group were excluded because more than 5% of their brain volumes contained movement-related artifacts. Finally, we tested for outliers in average whole-brain diffusion measures at time 1, time 2, and in change between time points, and excluded one participant in the trained group for showing a decrease in MD and RD that was greater than 2 standard deviations lower than the mean across both groups. Thus, our final dataset included DTI data at two time points for 23 trained individuals and 22 controls.

Behavioral Data

During the first testing session, we administered the Young Adult Self Report (Achenbach, 1990) to screen out participants who scored in the clinical range. We also administered two scales from the Wechsler Adult Scale of Intelligence (WASI; Wechsler, 1999), Matrix Reasoning and Vocabulary, to match the groups on IQ (see Table 5.1). During both testing sessions, we administered the Perceived Stress Scale (Cohen, 1983) and asked participants to

report their sleep schedules for the preceding two weeks. Reported stress levels and hours of sleep did not differ between groups at either time point (*Ps* > .4), and neither group changed significantly between time points (*Ps* > .2).

Training Paradigm

We selected the Blueprint Test Preparation course as the training paradigm because it provided more classroom time than other local programs: 100 hours distributed across the three components of the LSAT (35 hours for Logic Games, 35 hours for Logical Reasoning, and 30 hours for Reading Comprehension). "Logic Game" questions require test takers to integrate a series of rules in order to sequence or group a set of items. "Logical Reasoning" questions ask them to determine the logical flaw in an argument, identify an assumption, or choose a statement that would strengthen or weaken an argument. The remaining 30 hours of class time were dedicated to "Reading Comprehension" questions that require test-takers to interpret short passages of text.

For the Logic Games section, students were taught to break down problems into the essential information and to use diagrams to represent and integrate rules. For the Logical Reasoning section, students were taught basic logic principles (such as *modus ponens* and *modus tollens*), as well as how to avoid common logical fallacies. Students attempted problems at home and then instructors worked through the problems in class, answering any questions students might have. Special attention was paid to keeping motivation levels high by making the content fun through relatable examples.

Four LSAT practice tests were administered throughout the course. Practice test scores were provided either by the participants or (with participants' consent) by the test preparation company. We compared the scores on each of the LSAT sections for the first and fourth practice test as an index of change from time 1 to time 2.

Voxel-based Morphometry Analysis

To rule out the possibility that gray matter changes associated with training could be misinterpreted as changes in DTI parameters, we performed voxel-based morphometry analyses on the structural data from the trained group using FSL 4.1 (Functional MRI of the Brain (FMRIB) Software Library; Smith et al., 2004; Ashburner & Friston, 2000; Good et al., 2001). Structural images were skull-stripped using BET (Smith, 2002), and tissue-type segmentation was carried out using FAST (FMRIB's Automated Segmentation Tool; Zhang, Brady, & Smith, 2001). Gray-matter partial volume images were then aligned to standard space using FLIRT (FMRIB's Linear Image Registration Tool ; Jenkinson & Smith, 2001; Jenkinson, Bannister, Brady, & Smith, 2002), followed by nonlinear registration using FNIRT (FMRIB'S Nonlinear Image Registration Tool; Andersson, Jenkinson, & Smith, 2007a, 2007b), which uses a b-spline representation of the registration warp field (Rueckert et al., 1999). The resulting images were averaged to create a study-specific template, to which the native grey matter images were then non-linearly re-registered. The registered partial volume images were then modulated (to correct for local expansion or contraction) by dividing by the Jacobian of the warp field. The modulated segmented images were then smoothed with an isotropic Gaussian kernel with a sigma of 4 mm. Finally, a voxel-wise paired t-test general linear model (GLM) comparing pre-training to post-

training data was applied using Randomise (Nichols & Holmes, 2002) with 5000 permutations, correcting for multiple comparisons at $P < .05$.

DTI Data Acquisition and Preprocessing

Data were acquired on a 3 Tesla Siemens Trio TIM MR scanner using a 12-channel head coil with a maximum gradient strength of 40 mT/m. Structural and functional scans were collected in a fixed sequence across subjects and across time points. Here, we report on only the DTI data. DTI data were acquired using echo-planar imaging (EPI; TR = 7900 ms; TE = 102 ms; 2.2 mm^3 isotropic voxels; 55 axial slices). Parallel acquisition (GRAPPA) was used with at an acceleration factor of 2. Seven non-diffusion-weighted directions and 64 diffusion-weighted directions were acquired with a b-value of 2000 s/mm^2, uniformly distributed across 64 gradient directions.

Analyses were performed using tools from FDT (FMRIB's Diffusion Toolbox, part of FSL 4.1; Smith et al., 2004; Woolrich et al., 2009). Brain volumes were skull-stripped using the Brain Extraction Tool (Smith, 2002). A 12-parameter affine registration to the b = 0 weighted volume was applied to correct for head motion and eddy current distortions introduced by the gradient coils, and the gradient directions were rotated accordingly. A diffusion tensor model was fitted to the data in a voxel-wise fashion to generate whole-brain maps of the axial and radial diffusivity (AD and RD), FA, and MD.

The first volume of our DTI acquisition had no diffusion weighting and was used to align the DTI scans at both time points to each other using a 12 parameter affine transformation and skull images to constrain the registration scaling using FLIRT (Jenkinson & Smith, 2001; Jenkinson et al., 2002). Both images were resampled into a space halfway between the two. This transformation was then applied to the FA maps and the aligned maps averaged to generate a subject-specific mid-space template. We subsequently non-linearly aligned these template FA maps into standard space using FNIRT (Andersson et al., 2007a, 2007b). Whole-brain MD, AD, and RD maps were aligned to standard space through application of the same two-step transform (linearly into subject-template space, then non-linearly into standard space).

A white matter mask was created from each subject's high resolution T1-weighted scan, after brain extraction, using FAST (Zhang, Brady, & Smith, 2001). This mask was transformed into the subject's DTI space by applying the inverse of the affine registration of the non-diffusion weighted volume to the high resolution image. Both the registration and calculations of the inverse transform used FLIRT (Jenkinson, Bannister, Brady, & Smith, 2002). Once in DTI space, the white matter masks were registered to subject-template space and combined (through multiplication) to create a subject-specific definition of white matter voxels.

DTI Analyses

We performed voxel-wise statistical analysis using TBSS (Tract-Based Spatial Statistics, Smith et al., 2006). After FA maps were aligned to standard space, the mean FA image was generated and thinned to produce a mean FA skeleton that represented the centers of all tracts common to the group. Each subject's aligned FA, AD, RD, and MD data were then projected onto this skeleton by finding the nearest maximum FA value for the individual. This projection step aims to remove the effect of cross-subject spatial variability that remains after the non-linear registration. Skeletonized difference images (time 2 - time 1) were created for each subject, and

the resulting data were fed into an unpaired t-test to compare the trained group to the control group. Voxel-wise cross-subject permutation-based nonparametric statistics were performed using Randomise (Nichols & Holmes, 2002) with 5000 permutations and threshold-free cluster enhancement to correct for multiple comparisons at $P < .05$ (Smith & Nichols, 2009). We used the same statistical approach to test for pre-training differences between groups (unpaired t-test of time 1 data).

To better characterize the anatomy of white matter showing an effect of training, we examined a recently developed tensor index used to identify regions of crossing fibers (Douaud et al., 2011): the mode of anisotropy (Ennis & Kindlmann, 2006). Regions with a positive mode have linear anisotropy, and are likely to be part of a highly directional tract. In contrast, regions with a low or negative mode can be described as having planar anisotropy, and are more likely to contain crossing fibers. We extracted mode of anisotropy values from voxels that were significant in the whole-brain analyses, as well as mode values across the entire white matter skeleton. Specifically, we extracted values from the average of all time 1 and time 2 mode maps after they had been registered into the standard space by following the same two-step registration process as described above. Histograms with a bin width of 0.01 were created using fslstats, an FSL tool (Smith et al., 2004). We used a Mann-Whitney *U*-test to investigate differences in the distributions of mode values within each of the results regions and the white matter skeleton.

We tested for correlations between LSAT improvement, as measured by the difference between the first and fourth practice test, and diffusion changes at the whole brain level following the approach described above. We then tested for brain-behavior correlations in the anatomical regions defined by the Johns Hopkins University White Matter Label Atlas (Mori, 2005). While we predicted correlations in frontoparietal white matter, we decided to perform an exploratory analysis because we considered that brain-behavior relationships might be most prominent in tracts less centrally involved in reasoning. Therefore, we tested all 48 labels and corrected all statistics for multiple comparisons using a randomization-based family-wise error correction (Nichols & Hayasaka, 2003).

White matter labels were nonlinearly registered to subject-template space (halfway between time 1 and time 2 for each subject, described above) using the inverse of the transform previously used to register subject data to standard space. Then, the average value of all voxels which lay within each ROI and the subject-specific white matter mask was extracted separately from each map. A difference measure was calculated by subtracting the average value for time 1 from the average value for time 2.

We also applied this process to calculate the average difference values for FA, AD, RD and MD in the voxels that reached significance in the whole brain analyses (see inset in Figure 5.1).

5.3 Results

Behavioral improvement

For participants for whom all 4 practice test scores were available ($n = 16$), training was associated with a gain of 9 points on the LSAT ($P < .001$, $df = 15$, $t = 6.59$). Subtest data was available for 13 participants. These participants improved significantly on the two reasoning

components of the test, Logic Games ($P < .01$, $df = 12$, $t = 3.21$) and Logical Reasoning ($P < .001$, $df = 12$, $t = 4.91$). They also improved slightly on Reading Comprehension ($P = .03$, $df = 12$, $t = 2.45$). LSAT improvement was significantly correlated with the reasoning subtest scores (LG: $R = .85$, $P = .0002$; LR: $R = .68$, P = .01), but not with RC ($R = .5$, $P = .08$), suggesting that changes in LSAT scores were driven by reasoning gains.

Changes in diffusion measures

The trained and control groups did not differ at time 1 on any of the diffusion measures (FA, RD, AD, and MD). The groups also did not differ on grey or white matter volume at either time 1 or time 2. Further, we did not observe a significant effect of training on grey/white matter classification within the trained group.

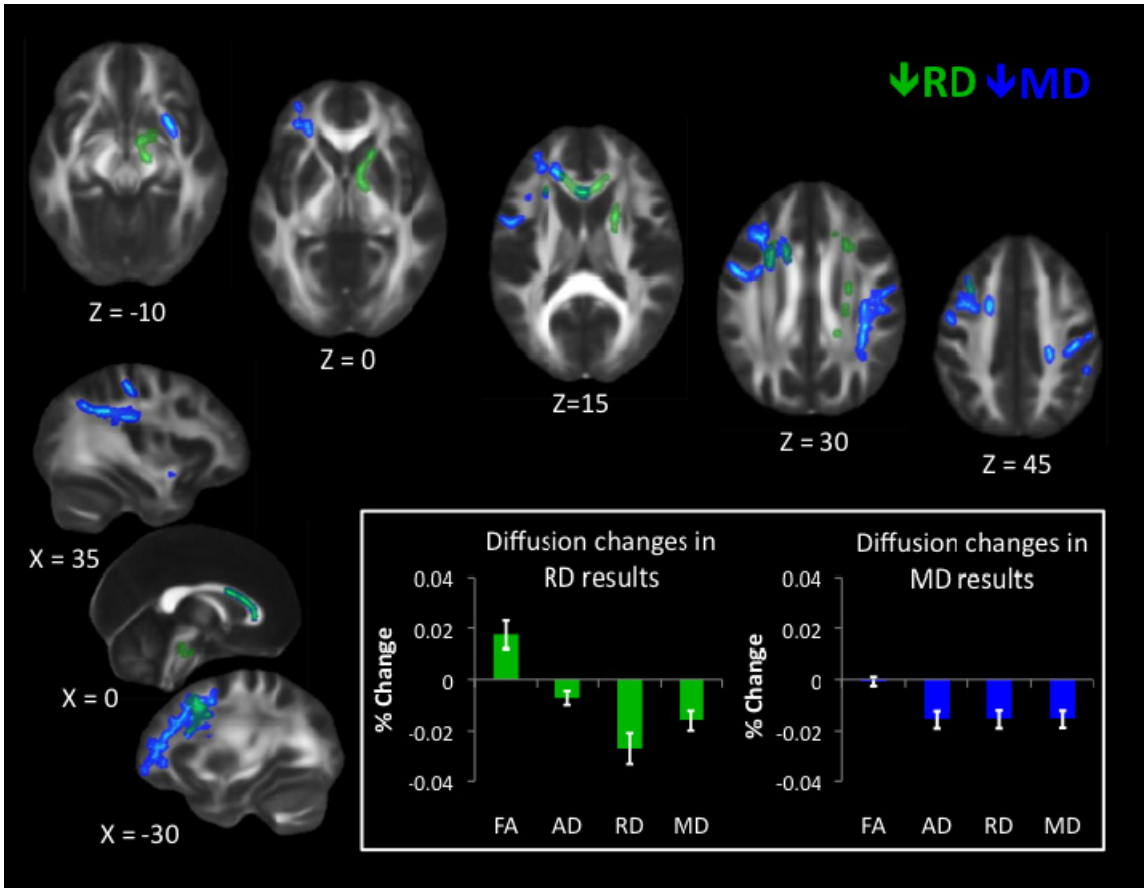

Figure 5.1: Results of whole-brain voxel-wise statistics. Decreases in RD are shown in green, and decreases in MD are shown in blue. Statistics were performed on skeletonized images, and results were filled for visualization purposes. Results are thresholded at $P < .05$, corrected for multiple comparisons with threshold-free cluster enhancement (Smith & Nichols, 2009). Inset shows percent change in diffusion measures extracted from voxels showing a significant decrease in RD (left) and MD (right) for the trained group only. Error bars represent standard error of the mean. No statistics are performed as they would be biased because values are extracted from voxels showing a significant change in diffusion at the whole brain level. The graph is meant to show qualitative differences in diffusion parameters between RD and MD results.

Whole-brain voxel-wise statistical analyses revealed significant decreases in RD and MD (but not in FA or AD) from time 1 to time 2 for the trained group compared to the control group, as described below. RD decreases were observed in white matter connecting frontal cortices (genu, anterior body of the corpus callosum, anterior corona radiata), and in descending white matter, including superior corona radiata, anterior internal capsule, and ventral brainstem (Figure 5.1, green). Training-related decreases in MD were generally more lateral, and closer to cortex, with the exception of decreases through anterior callosum (Figure 5.1, blue). MD decreases were particularly notable in white matter underlying left frontal cortex, including left RLPFC (see Figure 5.1, Z = 0), and right parietal cortex (Figure 5.1, Z = 30, X = 35).

When we extracted all four diffusion measures (FA, AD, RD, and MD) for the trained group from the voxels showing significant changes in RD (Figure 5.1, inset, left) and MD (Figure 5.1, inset, right), different patterns emerged. On average, voxels showing a decrease in RD also showed an increase in FA, which was likely not significant at the whole-brain level because of a slight concomitant decrease in AD. In contrast, voxels showing a significant decrease in MD showed roughly equal decreases in AD and RD, and therefore, no trend towards a change in FA.

Table 5.2: Locations of voxels showing RD decreases. Voxels are 1 mm^3. L = left, R= right

White Matter Label	Number of voxels
Anterior limb of internal capsule, R	526
Genu of corpus callosum	332
Superior corona radiata, R	254
Body of corpus callosum	178
Cerebral peduncle, R	178
Anterior corona radiata, R	172
Superior corona radiata, L	170
Anterior corona radiata, L	136
Corticospinal tract, R	133
Posterior limb of internal capsule, R	75
Superior cerebellar peduncle, R	68
Superior fronto-occipital fasciculus, R	67
Middle cerebellar peduncle	54
Posterior corona radiata, R	41
Pontine crossing tract	37
Splenium of corpus callosum	37
Medial lemniscus, R	13
Superior longitudinal fasciculus, R	5
External capsule, R	2
Total labeled voxels	2478
Total voxels	2912

Locations of RD and MD changes according to the JHU White Matter Label Atlas (Mori, 2005) are shown in Tables 4.2 and 4.3, respectively. While 85% of the voxels showing a decrease in RD were classified by the JHU atlas, only 35% of the voxels showing a decrease in MD fell into a white matter label, likely because this atlas classifies primarily deep white matter and not white matter

nearer to cortex. Importantly, because TBSS analyses test voxels along a white matter skeleton, we tested only voxels that were solidly in white matter, and not those contaminated by gray matter.

Table 5.3: Locations of voxels showing MD decreases. Voxels are 1 mm^3. L = left, R= right.

White Matter Label	Number of voxels
Anterior corona radiata, L	468
Superior corona radiata, L	299
Superior longitudinal fasciculus, R	266
Genu of corpus callosum	253
Body of corpus callosum	224
Superior longitudinal fasciculus, L	100
External capsule, R	99
Superior corona radiata, R	37
Uncinate fasciculus, R	13
Anterior limb of internal capsule, L	3
Superior fronto-occipital fasciculus, L	1
Total labeled voxels	1763
Total voxels	4989

In addition to an apparent difference in spatial distribution, we were interested to know whether the distribution of mode of anisotropy, a proxy measure for the presence of crossing fibers, differed between voxels showing a significant decrease in RD and MD. Figure 4.2 shows histograms of mode values for voxels showing changes in RD (green) and MD (blue). Mode values for the entire white matter skeleton are shown for comparison (black). Voxels showing a decrease in RD have an average mode ($M = 0.61$) that is significantly greater than the average mode of the white matter skeleton ($M = 0.47$, *Mann-Whitney* $U = 1.19 \times 10^{8}$, $df = 121805$, $P = 1.35 \times 10^{-186}$), providing evidence that RD changes occurred in highly directional tracts. In contrast, voxels showing a decrease in MD have an average mode slightly lower than the whole white matter skeleton ($M = 0.43$, $U = 2.78 \times 10^{8}$, $df = 123882$, $P = 2.93 \times 10^{-21}$), suggesting that MD changes were more likely to occur in regions with crossing fibers. The peak in mode values above 0.9 comes principally from voxels in the anterior callosum. Importantly, only 5% of RD results and 6% of MD results have a negative mode, so excluding these voxels from the analysis because they were not fit well by the standard linear tensor would not appreciably alter the results.

Diffusion-behavior correlations

We tested for significant correlations between behavioral improvement and diffusion changes at the whole-brain level, but did not find significant results ($P > .05$ corrected for multiple comparisons). We then tested for correlations between diffusion and LSAT improvement within ROIs defined from the JHU White Matter Atlas. This analysis revealed a significant negative correlation between change in MD and change in LSAT score in the retrolenticular part of the right internal capsule (Figure 4.3, Spearman's rho = -.667, P(uncorrected) = .005). This correlation was significant after a randomization -based family-wise error correction for 48 comparisons (Nichols & Hayasaka, 2003), as we tested each of the regions in the JHU White Matter Label Atlas (P(corrected) = .02).

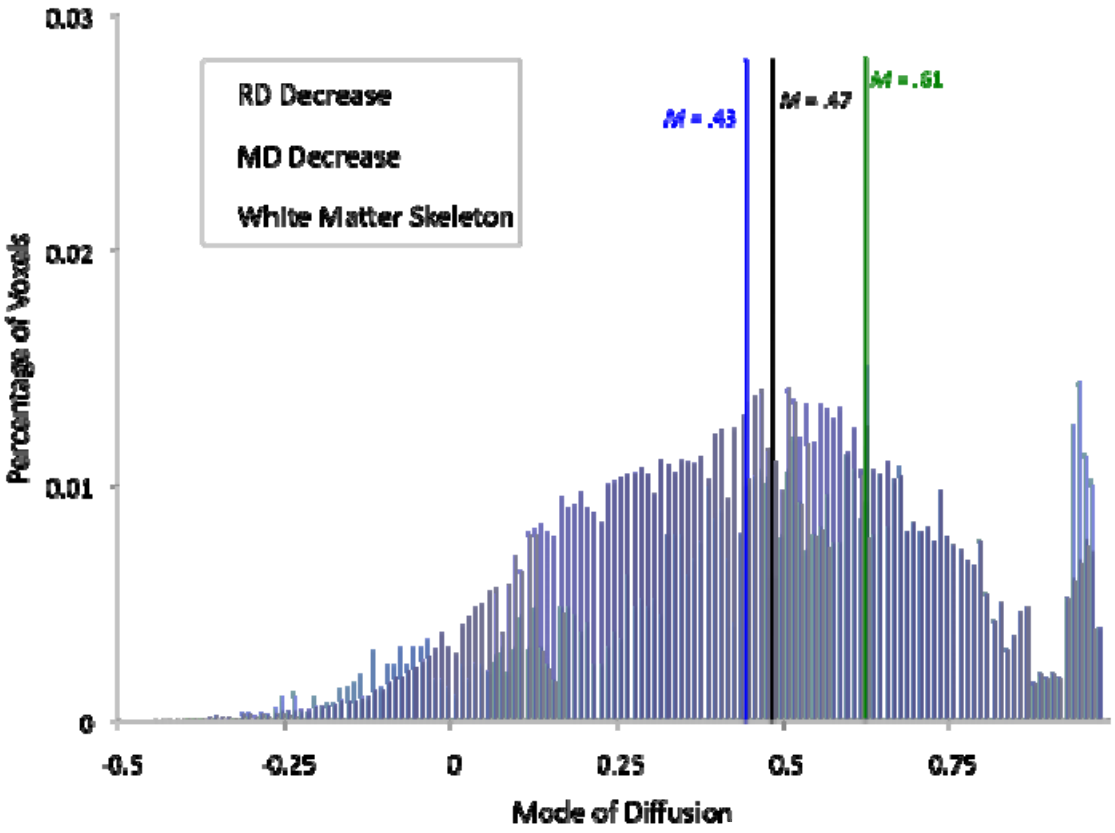

Figure 5.2: Distribution of diffusion mode for whole-brain results. Histograms showing percentage of voxels with a given mode value were calculated for voxels that exhibited a significant training effect at the whole-brain level in RD (green) or MD (blue). For comparison, a histogram of mode values for the entire white matter skeleton is shown (black). Mean mode for each set of voxels is marked by a vertical line (RD: green, MD: blue, white matter skeleton: black).

5.4 Discussion

In this study, we sought to test whether three months of reasoning training altered white matter microstructure. While we found no changes in white matter volume, we observed training-related changes in diffusion parameters within white matter. Indeed, our results show that reasoning training led to decreased RD in white matter connecting frontal cortices, and decreased in MD in white matter underlying left frontal and right parietal cortices. These experience-dependent changes fall into tracts that would be predicted by prior work showing that reasoning relies on an interhemispheric frontoparietal network (for review, see Prado et al., 2011). Our findings are also consistent with the view that reasoning is largely left-hemisphere dominent (e.g. Krawczyk, 2012), but that homologous cortex in the right hemisphere can be recruited as needed to support complex reasoning. Perhaps learning to reason more efficiently involves recruiting compensatory neural circuitry more consistently.

Relationships between diffusion changes and LSAT changes were not particularly robust, perhaps because neuroplastic changes were driven by experience shared across individuals. We found an unpredicted negative correlation between change in MD and improvement on the LSAT in the retrolenticular part of the right internal capsule (white matter that interconnects posterior cortices and thalamus) as well as corticopontine fibers originating in the right parietal lobe (Nolte, 2009). Future research with a larger sample size will be needed to determine whether these brain-behavior correlations are replicable, and whether there are any additional statistically significant relationships between diffusion change and reasoning improvement.

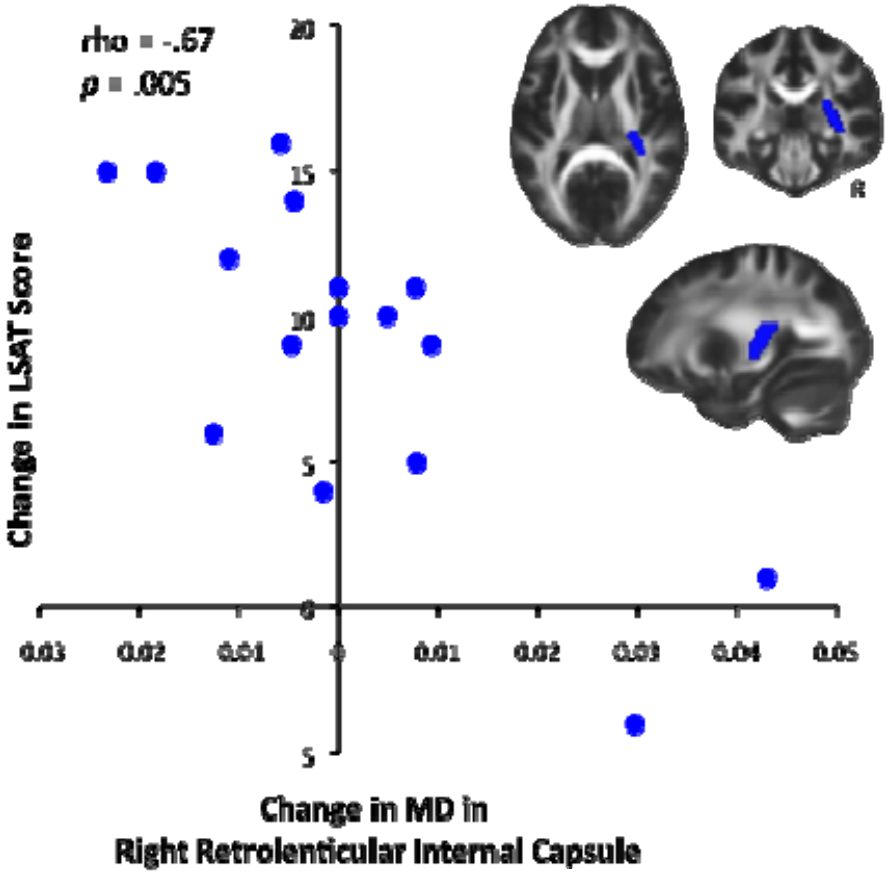

Figure 5.3: Correlation between LSAT improvement and MD decrease. LSAT change and MD change were significantly negatively correlated (Spearman's rho = -.667, *P*(uncorrected) = .005, *P*(corrected) = .02) in the right retrolenticular part of the internal capsule, an anatomical ROI defined from the JHU Label Atlas. Slices shown are: X = 27, Y = -29, Z = 10.

The results featured here meet a more conservative criterion than several prior training studies, in that changes in the trained group needed to surpass changes in the control group to be considered significant. The participants in our study were, on average, in their early twenties, and developmental changes in white matter are known to occur during this age range (Lebel, Walker, Leemans, Phillips, & Beaulieu, 2008). Additionally, both groups consisted largely of university students, and their academic experiences over the course of three months alone could have altered their white matter microstructure. Thus, changes that were significantly greater in the trained group than in a well-matched control group provide strong evidence for experience-dependent plasticity, and not simply maturational changes.

An active control group is often preferable to a passive control group in training studies, because it controls for general factors like beliefs about how much one is learning or improving on a task. For this study, however, selecting an appropriate active control group for this study would have been difficult as most adults would not choose to spend 100 hours over 3 months training on a skill that is not directly relevant to their life goals. Had we administered an artificial active control training program in the lab, differences between groups in neuroanatomical changes could have been confounded by differences in levels of motivation and attention. Alternatively, if our control group had consisted of individuals enrolled in a different professional training course, such as the Medical College Admissions Test (MCAT), we might have encountered initial group differences based on differences in interests, coursework, and experiences that would predispose students to seek admission to one professional program over another.

In this paper, we have examined changes in four measures of diffusion. On the one hand, this broad approach introduces a multiple comparison problem that would not exist if we had simply investigated changes in a single measure. On the other hand, if we had only looked at one measure, we would have painted a limited picture of white matter plasticity. Further, we did not have strong reason to believe that one index of white matter microstructure was more important or more likely to change with training than the others.

It is important to recognize that a tract defined by an atlas does not necessarily reflect an individual's anatomical tract. Rather, it reflects where tracts lie on average across individuals. At the current resolution, it is not possible to determine whether any given voxel contains axons connecting, for example, bilateral motor cortices or frontal and parietal cortices. Advances in diffusion imaging, such as diffusion spectral imaging (DSI), may make it possible to better classify the principal direction(s) of each voxel that shows a quantified change in diffusion. However, these sequences have yet to be used in the context of research on neuroplasticity. As the required scan time for advanced diffusion imaging pulse sequences decreases, and as scanners employ stronger gradients, it should become feasible to include more sensitive measures of white matter microstructure in studies of neuroplasticity that involve multiple structural and functional brain scans.

Even with advances in imaging methodology that make it possible to determine the direction of diffusion precisely, the study of white matter plasticity in humans will still be limited by the scale at which we can observe neuroanatomical changes. The cellular basis for training-induced changes in diffusion in humans is and will remain unclear, at least for the foreseeable future, though it is possible to speculate about potential mechanisms based on plasticity observed in animals (see Zatorre, Fields, & Johansen-Berg, 2012 for review).

Studies in animals have shown that both decreased RD and increased FA are related to increased myelination (Blumenfeld-Katzir, Pasternak, Dagan, & Assaf, 2011; Vorísek & Syková, 1997; Zhang et al., 2009). It is possible, then, that the experience-dependent decreases in RD (and increases in FA) that we observed were driven by myelination, especially because they tended to be in highly directional, heavily myelinated tracts. However, it is important to note that while myelin does affect diffusion (Concha, Livy, Beaulieu, Wheatley, & Gross, 2010; Mottershead et al., 2003), unmyelinated axon membranes do as well (Partridge et al., 2004), and myelin volume

and axon counts are very highly correlated (Concha et al., 2010; Schmierer et al., 2007). Therefore, the extent to which axonal cell membranes also constrain diffusion is unclear.

Decreased MD, on the other hand, has been related to proliferation and/or growth of astrocytes (Blumenfeld, Preminger, Sagi, & Tsodyks, 2006). A reduction in MD could additionally or alternatively reflect the myelination of axons traveling in multiple directions. It is therefore intriguing that we observed decreased MD near cortex, and also in white matter that was not highly directional and therefore could contain crossing fibers. Hopefully, future research linking changes in cell structure and function to plasticity in large-scale networks will further our understanding of how experience shapes the anatomy of the human brain.

Chapter 6: Conclusion

Author contribution statement

Kirstie Whitaker: Wrote the manuscript.

This dissertation presents four aspects of my graduate work, all of which have focused on elucidating the connections between white matter integrity (WMI) and cognition within individuals. The individual differences analyses that these studies employed allow for wide applicability of the findings to larger populations. I hope that each of the studies will inform and inspire future work with clinical applications.

The first study (chapter two) used a longitudinal data set to investigate *within-person* changes in white matter integrity and reasoning ability (RA). In this cohort, initial WMI was not correlated with the individual's gains in RA over time (afer the effects of age were accounted for). However, the amount that the participant's brain *changed* over time strongly predicted their gains in RA. There has been ample evidence that the brain is still maturing during childhood and adolescence (for example: Lebel, Walker, Leemans, Phillips, & Beaulieu, 2008). These results support the need for additional longitudinal studies that measure changes in the same individual over time. Our understanding of the brain is significantly enhanced by measuring individual variability over development, as it no longer needs to be limited to measurements of gross absolute changes over childhood and adolescence. It is not only the absolute values that inform our understanding of brain development, but also the journey through childhood and adolescence. This study supports a hypothesis that some childhood psychiatric illnesses may be caused by deviations from the typical trajectory in the timing of brain development.

In chapter three, my co-authors and I used structural equation modeling (SEM) to show the mediation of the relationship between WMI and RA by cognitive processing speed. Reasoning is such a complicated process that advanced statistical analyses are necessary if we are to consider all of the factors which relate brain to behavior. There are many future directions that I hope this work will inspire, not least of which is to advance the use of SEM in studies relating cognition to the brain. We only investigated a few white matter regions of interest, and found that global WMI predicting processing speed which in turn predicted RA was the most parsimonious result. However, future studies of our longitudinal cohort will allow us to further characterize the dynamic interaction between structural changes in the brain and changes in cognition over age.

While the first two studies investigated children and adolescents during development, the third study (chapter four) focused on two groups of adults who had experienced different perceptual environments during childhood and adolescence: grapheme-color synesthetes and non-synesthete control participants. In this study, we found that synesthetes had globally different white matter integrity when compared to the control group. Additionally, in the synesthete group, there was a clear relationship between individual differences in WMI and vividness of visual imagery, when compared to controls. A clear avenue of future inquiry is to study the white matter of synesthetic children: do the disparities between synesthetes and non-synesthetes exist from an early age, or do they develop over time?

The final study in this dissertation (chapter five) asked whether white matter changes in response to an intervention. We found that, in response to three months of reasoning training, certain measures of WMI changed in white matter underlying fronto-partietal cortices and in interhemispheric connections. Additionally, individual differences in white matter changes in the right internal capsule predicted the participants' gains on the law school admissions test. This study required rigorous methodological consideration, and a complex analysis pipeline. For example, our analyses involved registering the same person's brain at two time points first to each other to generate a subject-specific template, and then to standard space. Additionally, we ensured that our results were in regions which showed a significantly larger change between the two scans than the change experienced by a non-trained control group. I hope that future studies of training effects on the brain maintain the rigor with which my co-authors and I have approached the analysis of this data.

These four studies have all investigated individual differences in brain structure and cognition. I have investigated typically developing children, both cross-sectionally and longitudinally, adults exposed to different developmental environments, and adults who have undergone rigorous cognitive training. However, a key component that future work must address is the relationship between these measures of brain structure and cognition to brain *function*. I have assumed throughout this dissertation that brain structure is related to cognitive ability, but have not directly tested this relationship. I hope that future work, by myself, my collaborators, and others, will integrate brain structure, function and cognitive abilities. I am excited to see the work presented in this dissertation inform these future studies: both in terms of understanding the effects of brain development on the emergence of complex cognition, and in terms of the plasticity of the brain in response to intervention.

References

Achenbach, T. M. (1990). *Young adult self report*. Burlington, VT: University of Vermont, Department of Psychiatry.

Achenbach, T. M. (1991). *Integrative guide for the 1991 CBCL/4-18, YSR and TRF profiles*. Burlington, VT: University of Vermont, Department of Psychiatry.

Aleman, A., Rutten, G. J., Sitskoorn, M. M., Dautzenberg, G., & Ramsey, N. F. (2001). Activation of striate cortex in the absence of visual stimulation: an fMRI study of synesthesia. *Neuroreport*, *12*(13), 2827–30. Retrieved from http://www.ncbi.nlm.nih.gov/pubmed/11588585

Andersson, J. L. R., Jenkinson, M., & Smith, S. M. (2007a). Non-linear optimisation FMRIB Technial Report TR07JA1. *In Practice*, (June).

Andersson, J. L. R., Jenkinson, M., & Smith, S. M. (2007b). Non-linear registration aka Spatial normalisation FMRIB Technial Report TR07JA2, (June).

Ashburner, J., & Friston, K. J. (2000). Voxel-based morphometry--the methods. *NeuroImage*, *11*(6 Pt 1), 805–21. Retrieved from http://www.ncbi.nlm.nih.gov/pubmed/10860804

Assaf, Y., & Pasternak, O. (2008). Diffusion tensor imaging (DTI)-based white matter mapping in brain research: a review. *J Mol Neurosci*, *34*(1), 51–61. doi:10.1007/s12031-007-0029-0

Baldo, J. V., Bunge, S. A., Wilson, S. M., & Dronkers, N. F. (2010). Is relational reasoning dependent on language? A voxel-based lesion symptom mapping study. *Brain and language*, *113*(2), 59–64. doi:10.1016/j.bandl.2010.01.004

Barnett, K. J., Foxe, J. J., Molholm, S., Kelly, S. P., Shalgi, S., Mitchell, K. J., & Newell, F. N. (2008). Differences in early sensory-perceptual processing in synesthesia: a visual evoked potential study. *NeuroImage*, *43*(3), 605–13. Retrieved from http://www.ncbi.nlm.nih.gov/pubmed/18723094

Barnett, K. J., & Newell, F. N. (2008). Synaesthesia is associated with enhanced, self-rated visual imagery. *Consciousness and cognition*, *17*(3), 1032–9. Retrieved from http://dx.doi.org/10.1016/j.concog.2007.05.011

Barres, B. A., & Raff, M. C. (1993). Proliferation of oligodendrocyte precursor cells depends on electrical activity in axons. *Nature*, *361*(6409), 258–60. doi:10.1038/361258a0

Basser, P. J. (1995). Inferring microstructural features and the physiological state of tissues from diffusion-weighted images. *NMR in biomedicine*, *8*(7-8), 333–44. Retrieved from http://www.ncbi.nlm.nih.gov/pubmed/8739270

Beaulieu, C. (2002). The basis of anisotropic water diffusion in the nervous system - a technical review. *NMR Biomed*, *15*(7-8), 435–455. doi:10.1002/nbm.782

Beeli, G., Esslen, M., & Jäncke, L. (2008). Time course of neural activity correlated with colored-hearing synesthesia. *Cerebral cortex (New York, N.Y. : 1991)*, *18*(2), 379–85. Retrieved from http://www.ncbi.nlm.nih.gov/pubmed/17573375

Behrens, T. E. J., Berg, H. J., Jbabdi, S., Rushworth, M. F. S., & Woolrich, M. W. (2007). Probabilistic diffusion tractography with multiple fibre orientations: What can we gain? *NeuroImage*, *34*(1), 144–55. Retrieved from http://www.ncbi.nlm.nih.gov/pubmed/17070705

Benes, F. M., Turtle, M., Khan, Y., & Farol, P. (1994). Myelination of a key relay zone in the hippocampal formation occurs in the human brain during childhood, adolescence, and adulthood. *Archives of general psychiatry*, *51*, 477–484. Retrieved from http://archpsyc.ama-assn.org/cgi/content/abstract/51/6/477

Blair, C. (2006). How similar are fluid cognition and general intelligence? A developmental neuroscience perspective on fluid cognition as an aspect of human cognitive ability. *The Behavioral and brain sciences*, *29*(2), 109–25; discussion 125–60. doi:10.1017/S0140525X06009034

Blumenfeld, B., Preminger, S., Sagi, D., & Tsodyks, M. (2006). Dynamics of memory representations in networks with novelty-facilitated synaptic plasticity. *Neuron*, *52*(2), 383–94. Retrieved from http://www.ncbi.nlm.nih.gov/pubmed/17046699

Blumenfeld-Katzir, T., Pasternak, O., Dagan, M., & Assaf, Y. (2011). Diffusion MRI of structural brain plasticity induced by a learning and memory task. *PloS one*, *6*(6), e20678. Retrieved from http://www.pubmedcentral.nih.gov/articlerender.fcgi?artid=3119075&tool=pmcentrez&rendertype=abstract

Brang, D., Hubbard, E. M., Coulson, S., Huang, M., & Ramachandran, V. S. (2010). Magnetoencephalography reveals early activation of V4 in grapheme-color synesthesia. *NeuroImage*, *53*(1), 268–74. Retrieved from http://www.ncbi.nlm.nih.gov/pubmed/20547226

Brang, D., Williams, L. E., & Ramachandran, V. S. (2012). Grapheme-color synesthetes show enhanced crossmodal processing between auditory and visual modalities. *Cortex; a journal devoted to the study of the nervous system and behavior*, *48*(5), 630–7. Retrieved from http://www.ncbi.nlm.nih.gov/pubmed/21763646

Braver, T. S., & Bongiolatti, S. R. (2002). The role of frontopolar cortex in subgoal processing during working memory. *NeuroImage*, *15*(3), 523–36. Retrieved from http://www.ncbi.nlm.nih.gov/pubmed/11848695

Bunge, S. A., Helskog, E. H., & Wendelken, C. (2009). Left, but not right, rostrolateral prefrontal cortex meets a stringent test of the relational integration hypothesis. *NeuroImage*, *46*(1), 338–42. doi:10.1016/j.neuroimage.2009.01.064

Bunge, S. A., Wendelken, C., Badre, D., & Wagner, A. D. (2005). Analogical reasoning and prefrontal cortex: evidence for separable retrieval and integration mechanisms. *Cerebral cortex*, *15*(3), 239–49. doi:10.1093/cercor/bhh126

Catani, M., & Ffytche, D. H. (2005). The rises and falls of disconnection syndromes. *Brain : a journal of neurology*, *128*(Pt 10), 2224–39. Retrieved from http://www.ncbi.nlm.nih.gov/pubmed/16141282

Cattell, R. B. (1971). *Abilities: Their structure, growth and action*. Boston, MA: Houghton-Miffin.

Cattell, R. B. (1987). *Intelligence: Its structure, growth and action*. New York, NY: Elsevier.

Charlton, R. a, Landau, S., Schiavone, F., Barrick, T. R., Clark, C. a, Markus, H. S., & Morris, R. G. (2008). A structural equation modeling investigation of age-related variance in executive function and DTI measured white matter damage. *Neurobiology of aging*, *29*(10), 1547–55. doi:10.1016/j.neurobiolaging.2007.03.017

Chiang, M.-C., Barysheva, M., Shattuck, D. W., Lee, A. D., Madsen, S. K., Avedissian, C., Klunder, A. D., et al. (2009). Genetics of brain fiber architecture and intellectual performance. *Journal of Neuroscience*, *29*(7), 2212–24. doi:10.1523/JNEUROSCI.4184-08.2009

Choi, Y. Y., Shamosh, N. A., Cho, S. H., DeYoung, C. G., Lee, M. J., Lee, J.-M., Kim, S. I., et al. (2008). Multiple bases of human intelligence revealed by cortical thickness and neural activation. *Journal of Neuroscience*, *28*(41), 10323–9. doi:10.1523/JNEUROSCI.3259-08.2008

Cohen, S. (1983). A global measure of perceived stress. *Journal of health and social …*. Retrieved from http://www.jstor.org/stable/10.2307/2136404

Concha, L., Livy, D. J., Beaulieu, C., Wheatley, B. M., & Gross, D. W. (2010). In vivo diffusion tensor imaging and histopathology of the fimbria-fornix in temporal lobe epilepsy. *J Neurosci*, *30*(3), 996–1002. doi:10.1523/JNEUROSCI.1619-09.2010

Crone, E. A., Wendelken, C., Donohue, S., van Leijenhorst, L., & Bunge, S. A. (2006). Neurocognitive development of the ability to manipulate information in working memory. *Proceedings of the National Academy of Sciences of the United States of America*, *103*(24), 9315–20. doi:10.1073/pnas.0510088103

Desikan, R. S., Ségonne, F., Fischl, B., Quinn, B. T., Dickerson, B. C., Blacker, D., Buckner, R. L., et al. (2006). An automated labeling system for subdividing the human cerebral cortex on MRI scans into gyral based regions of interest. *NeuroImage*, *31*(3), 968–80. doi:10.1016/j.neuroimage.2006.01.021

Douaud, G., Jbabdi, S., Behrens, T. E. J., Menke, R. A., Gass, A., Monsch, A. U., Rao, A., et al. (2011). DTI measures in crossing-fibre areas: increased diffusion anisotropy reveals early white matter alteration in MCI and mild Alzheimer's disease. *Neuroimage*, *55*(3), 880–890. doi:10.1016/j.neuroimage.2010.12.008

Dovern, A., Fink, G. R., Fromme, A. C. B., Wohlschläger, A. M., Weiss, P. H., & Riedl, V. (2012). Intrinsic network connectivity reflects consistency of synesthetic experiences. *The Journal of neuroscience : the official journal of the Society for Neuroscience*, *32*(22), 7614–21. Retrieved from http://www.ncbi.nlm.nih.gov/pubmed/22649240

Dumontheil, I., Houlton, R., Christoff, K., & Blakemore, S.-J. (2010). Development of relational reasoning during adolescence. *Developmental science*, *13*(6), F15–24. doi:10.1111/j.1467-7687.2010.01014.x

Eagleman, D. M., Kagan, A. D., Nelson, S. S., Sagaram, D., & Sarma, A. K. (2007). A standardized test battery for the study of synesthesia. *Journal of neuroscience methods*, *159*(1), 139–45. Retrieved from http://www.ncbi.nlm.nih.gov/pubmed/16919755

Elias, L. J., Saucier, D. M., Hardie, C., & Sarty, G. E. (2003). Dissociating semantic and perceptual components of synaesthesia: behavioural and functional neuroanatomical investigations. *Brain research. Cognitive brain research*, *16*(2), 232–7. Retrieved from http://www.ncbi.nlm.nih.gov/pubmed/12668232

Engel, A. K., Fries, P., & Singer, W. (2001). Dynamic predictions: oscillations and synchrony in top-down processing. *Nature reviews. Neuroscience*, *2*(10), 704–16. Retrieved from http://www.ncbi.nlm.nih.gov/pubmed/11584308

Ennis, D. B., & Kindlmann, G. (2006). Orthogonal tensor invariants and the analysis of diffusion tensor magnetic resonance images. *Magn Reson Med*, *55*(1), 136–146. doi:10.1002/mrm.20741

Eslinger, P. J., Blair, C., Wang, J., Lipovsky, B., Realmuto, J., Baker, D., Thorne, S., et al. (2009). Developmental shifts in fMRI activations during visuospatial relational reasoning. *Brain and cognition*, *69*(1), 1–10. Retrieved from http://www.ncbi.nlm.nih.gov/pubmed/18835075

Esterman, M., Verstynen, T., Ivry, R. B., & Robertson, L. C. (2006). Coming unbound: disrupting automatic integration of synesthetic color and graphemes by transcranial magnetic stimulation of the right parietal lobe. *Journal of cognitive neuroscience*, *18*(9), 1570–6. Retrieved from http://www.ncbi.nlm.nih.gov/pubmed/16989556

Ferrer, E., & McArdle, J. J. (2004). An experimental analysis of dynamic hypotheses about cognitive abilities and achievement from childhood to early adulthood. *Developmental psychology*, *40*(6), 935–52. Retrieved from http://www.ncbi.nlm.nih.gov/pubmed/15535749

Ferrer, E., O'Hare, E. D., & Bunge, S. a. (2009). Fluid reasoning and the developing brain. *Frontiers in neuroscience*, *3*(1), 46–51. doi:10.3389/neuro.01.003.2009

Fry, A. F., & Hale, S. (2000). Relationships among processing speed, working memory, and fluid intelligence in children. *Biological psychology*, *54*(1-3), 1–34. Retrieved from http://www.ncbi.nlm.nih.gov/pubmed/11035218

Good, C. D., Johnsrude, I. S., Ashburner, J., Henson, R. N., Friston, K. J., & Frackowiak, R. S. (2001). A voxel-based morphometric study of ageing in 465 normal adult human brains. *NeuroImage*, *14*(1 Pt 1), 21–36. Retrieved from http://www.ncbi.nlm.nih.gov/pubmed/11525331

Goswami, U. (1992). *Analogical Reasoning in Children* (p. 156). Hillsdale, NJ: L. Erlbaum. Retrieved from http://books.google.com/books?id=bNNBc_zgsNsC&pgis=1

Gottfredson, L. S. (1997). Why g matters: The complexity of everyday life. *Intelligence*, *24*(1), 79–132. doi:10.1016/S0160-2896(97)90014-3

Gray, J. R., Chabris, C. F., & Braver, T. S. (2003). Neural mechanisms of general fluid intelligence. *Nature Neuroscience*, *6*(3), 316–22. doi:10.1038/nn1014

Gutiérrez, R., Boison, D., Heinemann, U., & Stoffel, W. (1995). Decompaction of CNS myelin leads to a reduction of the conduction velocity of action potentials in optic nerve. *Neuroscience letters*, *195*(2), 93–6. Retrieved from http://www.ncbi.nlm.nih.gov/pubmed/7478276

Hagmann, P., Cammoun, L., Gigandet, X., Meuli, R., Honey, C. J., Wedeen, V. J., & Sporns, O. (2008). Mapping the structural core of human cerebral cortex. *PLoS biology*, *6*(7), e159. Retrieved from http://www.pubmedcentral.nih.gov/articlerender.fcgi?artid=2443193&tool=pmcentrez&rendertype=abstract

Hampshire, A., Thompson, R., Duncan, J., & Owen, A. M. (2011). Lateral prefrontal cortex subregions make dissociable contributions during fluid reasoning. *Cerebral cortex*, *21*(1), 1–10. doi:10.1093/cercor/bhq085

Horn, J. L. (1991). Measurement of intellectual capabilities: a review of theory. In K S McGrew, J. K. Werder, & R. W. Woodcock (Eds.), *Woodcock-Johnson Technical Manual*. Allen, TX: DLM Teaching Resources.

Hubbard, E. M., Arman, A. C., Ramachandran, V. S., & Boynton, G. M. (2005). Individual differences among grapheme-color synesthetes: brain-behavior correlations. *Neuron*, *45*(6), 975–85. Retrieved from http://www.ncbi.nlm.nih.gov/pubmed/15797557

Hupé, J.-M., Bordier, C., & Dojat, M. (2012). The neural bases of grapheme-color synesthesia are not localized in real color-sensitive areas. *Cerebral cortex (New York, N.Y. : 1991)*, *22*(7), 1622–33. Retrieved from http://www.ncbi.nlm.nih.gov/pubmed/21914631

Hänggi, J., Wotruba, D., & Jäncke, L. (2011). Globally altered structural brain network topology in grapheme-color synesthesia. *The Journal of neuroscience : the official journal of the Society for Neuroscience*, *31*(15), 5816–28. Retrieved from http://www.ncbi.nlm.nih.gov/pubmed/21490223

Imfeld, A., Oechslin, M. S., Meyer, M., Loenneker, T., & Jancke, L. (2009). White matter plasticity in the corticospinal tract of musicians: a diffusion tensor imaging study. *NeuroImage*, *46*(3), 600–7. Retrieved from http://www.ncbi.nlm.nih.gov/pubmed/19264144

Jansari, A. S., Spiller, M. J., & Redfern, S. (2006). Number synaesthesia: when hearing "four plus five" looks like gold. *Cortex; a journal devoted to the study of the nervous system and behavior*, *42*(2), 253–8. Retrieved from http://www.ncbi.nlm.nih.gov/pubmed/16683499

Jenkinson, M., Bannister, P., Brady, M., & Smith, S. M. (2002). Improved Optimization for the Robust and Accurate Linear Registration and Motion Correction of Brain Images. *NeuroImage*, *17*(2), 825–841. doi:10.1006/nimg.2002.1132

Jenkinson, M., & Smith, S. M. (2001). A global optimisation method for robust affine registration of brain images. *Medical image analysis*, *5*(2), 143–56. Retrieved from http://www.ncbi.nlm.nih.gov/pubmed/11516708

Jung, R. E., & Haier, R. J. (2007). The Parieto-Frontal Integration Theory (P-FIT) of intelligence: converging neuroimaging evidence. *Behav Brain Sci*, *30*(2), 135–187. doi:10.1017/S0140525X07001185

Jäncke, L., & Langer, N. (2011). A strong parietal hub in the small-world network of coloured-hearing synaesthetes during resting state EEG. *Journal of neuropsychology*, *5*(2), 178–202. Retrieved from http://www.ncbi.nlm.nih.gov/pubmed/21923785

Kail, R. (1991). Developmental change in speed of processing during childhood and adolescence. *Psychological bulletin*, *109*(3), 490–501. Retrieved from http://www.ncbi.nlm.nih.gov/pubmed/2062981

Kail, R., & Salthouse, T. A. (1994). Processing speed as a mental capacity. *Acta psychologica*, *86*(2-3), 199–225. Retrieved from http://www.ncbi.nlm.nih.gov/pubmed/7976467

Krawczyk, D. C. (2012). The cognition and neuroscience of relational reasoning. *Brain research*, *1428*(null), 13–23. doi:10.1016/j.brainres.2010.11.080

Lebel, C., & Beaulieu, C. (2011). Longitudinal Development of Human Brain Wiring Continues from Childhood into Adulthood. *Journal of Neuroscience*, *31*(30), 10937–10947. doi:10.1523/JNEUROSCI.5302-10.2011

Lebel, C., Walker, L., Leemans, A., Phillips, L., & Beaulieu, C. (2008). Microstructural maturation of the human brain from childhood to adulthood. *NeuroImage*, *40*(3), 1044–55. doi:10.1016/j.neuroimage.2007.12.053

Li, S.-C., Lindenberger, U., Hommel, B., Aschersleben, G., Prinz, W., & Baltes, P. B. (2004). Transformations in the couplings among intellectual abilities and constituent cognitive processes across the life span. *Psychological science*, *15*(3), 155–63. Retrieved from http://www.ncbi.nlm.nih.gov/pubmed/15016286

Locke, J. (1689). *An essay concerning human understanding*. London: Dent.

Mackey, A. P., Whitaker, K. J., & Bunge, S. A. (n.d.). Experience-dependent plasticity in white matter microstructure: reasoning training alters structural connectivity. *Frontiers in Neuroanatomy*, *in press*.

Marks, D. (1973). Visual imagery in the recall of pictures. *British Journal of Psychology*, (64), 17–24.

McArdle, J. J., Ferrer-Caja, E., Hamagami, F., & Woodcock, R. W. (2002). Comparative longitudinal structural analyses of the growth and decline of multiple intellectual abilities over the life span. *Developmental psychology*, *38*(1), 115–42. doi:10.1037/0012-1649.38.1.115

McGrew, Kevin S, Werder, J. K., & Woodcock, R. W. (1991). *WJ-R technical manual*. Itasca, IL: Riverside Publishing.

Mechelli, A., Price, C. J., Friston, K. J., & Ishai, A. (2004). Where bottom-up meets top-down: neuronal interactions during perception and imagery. *Cerebral cortex (New York, N.Y. : 1991)*, *14*(11), 1256–65. Retrieved from http://www.ncbi.nlm.nih.gov/pubmed/15192010

Mori, S. (2005). *MRI Atlas of Human White Matter*. Amsterdam: Elsevier.

Mori, S., & Zhang, J. (2006). Principles of diffusion tensor imaging and its applications to basic neuroscience research. *Neuron*, *51*(5), 527–39. doi:10.1016/j.neuron.2006.08.012

Moseley, M., Bammer, R., & Illes, J. (2002). Diffusion-tensor imaging of cognitive performance. *Brain and cognition*, *50*(3), 396–413. doi:10.1016/S0278-2626(02)00524-9

Mottershead, J. P., Schmierer, K., Clemence, M., Thornton, J. S., Scaravilli, F., Barker, G. J., Tofts, P. S., et al. (2003). High field MRI correlates of myelin content and axonal density in multiple sclerosis--a post-mortem study of the spinal cord. *Journal of neurology*, *250*(11), 1293–301. doi:10.1007/s00415-003-0192-3

Muggleton, N., Tsakanikos, E., Walsh, V., & Ward, J. (2007). Disruption of synaesthesia following TMS of the right posterior parietal cortex. *Neuropsychologia*, *45*(7), 1582–5. Retrieved from http://www.ncbi.nlm.nih.gov/pubmed/17222433

Mulvenna, C. M., Hubbard, E. M., Ramachandran, V. S., & Pollick, E. (2003). *The relationship between synaesthesia and creativity*. Glasgow: University of Glasgow.

Muthen, L. K., & Muthen, B. O. (1998). *MPlus User's Guide*. Los Angeles: Muthen & Muthen.

Neufeld, J., Sinke, C., Zedler, M., Dillo, W., Emrich, H. M., Bleich, S., & Szycik, G. R. (2012). Disinhibited feedback as a cause of synesthesia: evidence from a functional connectivity study on auditory-visual synesthetes. *Neuropsychologia*, *50*(7), 1471–7. Retrieved from http://www.ncbi.nlm.nih.gov/pubmed/22414594

Nichols, T. E., & Hayasaka, S. (2003). Controlling the familywise error rate in functional neuroimaging: a comparative review. *Statistical methods in medical research*, *12*(5), 419–46. Retrieved from http://www.ncbi.nlm.nih.gov/pubmed/14599004

Nichols, T. E., & Holmes, A. P. (2002). Nonparametric permutation tests for functional neuroimaging: a primer with examples. *Human brain mapping*, *15*(1), 1–25. Retrieved from http://www.ncbi.nlm.nih.gov/pubmed/11747097

Nolte, J. (2009). *The Human Brain: An Introduction to its Functional Anatomy* (6th ed.). Philadelphia, PA: Mosby Elsevier.

Nunn, J. A., Gregory, L. J., Brammer, M., Williams, S. C. R., Parslow, D. M., Morgan, M. J., Morris, R. G., et al. (2002). Functional magnetic resonance imaging of synesthesia: activation of V4/V8 by spoken words. *Nature neuroscience*, *5*(4), 371–5. Retrieved from http://www.ncbi.nlm.nih.gov/pubmed/11914723

Partridge, S. C., Mukherjee, P., Henry, R. G., Miller, S. P., Berman, J. I., Jin, H., Lu, Y., et al. (2004). Diffusion tensor imaging: serial quantitation of white matter tract maturity in premature newborns. *Neuroimage*, *22*(3), 1302–1314. doi:10.1016/j.neuroimage.2004.02.038

Paulesu, E., Harrison, J., Baron-Cohen, S., Watson, J. D., Goldstein, L., Heather, J., Frackowiak, R. S., et al. (1995). The physiology of coloured hearing. A PET activation study of colour-word synaesthesia. *Brain : a journal of neurology*, *118 (Pt 3*, 661–76. Retrieved from http://www.ncbi.nlm.nih.gov/pubmed/7600084

Pierpaoli, C., & Basser, P. J. (1996). Toward a quantitative assessment of diffusion anisotropy. *Magnetic resonance in medicine : official journal of the Society of Magnetic Resonance in Medicine / Society of Magnetic Resonance in Medicine*, *36*(6), 893–906. Retrieved from http://www.ncbi.nlm.nih.gov/pubmed/8946355

Prado, J., Chadha, A., & Booth, J. R. (2011). The brain network for deductive reasoning: a quantitative meta-analysis of 28 neuroimaging studies. *Journal of cognitive neuroscience*, *23*(11), 3483–97. Retrieved from http://www.pubmedcentral.nih.gov/articlerender.fcgi?artid=3188687&tool=pmcentrez&rendertype=abstract

Price, M. C. (2009). What kind of mental images are spatial forms? *Cognitive processing*, *10 Suppl 2*, S276–8. Retrieved from http://www.ncbi.nlm.nih.gov/pubmed/19693588

Raven, J. C. (1938). Standardization of progressive matrices. *British Journal of Medical Psychology*, *19*(1), 137–150. Retrieved from http://doi.wiley.com/10.1111/j.2044-8341.1941.tb00316.x

Rich, A. N., Williams, M. A., Puce, A., Syngeniotis, A., Howard, M. A., McGlone, F., & Mattingley, J. B. (2006). Neural correlates of imagined and synaesthetic colours. *Neuropsychologia*, *44*(14), 2918–25. Retrieved from http://www.ncbi.nlm.nih.gov/pubmed/16901521

Richland, L. E., Morrison, R. G., & Holyoak, K. J. (2006). Children's development of analogical reasoning: insights from scene analogy problems. *Journal of experimental child psychology*, *94*(3), 249–73. doi:10.1016/j.jecp.2006.02.002

Roberts, R. E., Anderson, E. J., & Husain, M. (2010). Expert cognitive control and individual differences associated with frontal and parietal white matter microstructure. *The Journal of neuroscience : the official journal of the Society for Neuroscience*, *30*(50), 17063–7. Retrieved from http://www.pubmedcentral.nih.gov/articlerender.fcgi?artid=3115511&tool=pmcentrez&rendertype=abstract

Robertson, L. C. (2003). Binding, spatial attention and perceptual awareness. *Nature reviews. Neuroscience*, *4*(2), 93–102. Retrieved from http://www.pubmedcentral.nih.gov/articlerender.fcgi?artid=3373472&tool=pmcentrez&rendertype=abstract

Rothen, N., & Meier, B. (2010). Grapheme-colour synaesthesia yields an ordinary rather than extraordinary memory advantage: evidence from a group study. *Memory (Hove, England)*, *18*(3), 258–64. Retrieved from http://www.ncbi.nlm.nih.gov/pubmed/20169501

Rothen, N., Nyffeler, T., von Wartburg, R., Müri, R., & Meier, B. (2010). Parieto-occipital suppression eliminates implicit bidirectionality in grapheme-colour synaesthesia.

Neuropsychologia, *48*(12), 3482–7. Retrieved from http://www.ncbi.nlm.nih.gov/pubmed/20678509

Rouw, R., & Scholte, H. S. (2007). Increased structural connectivity in grapheme-color synesthesia. *Nature neuroscience*, *10*(6), 792–7. Retrieved from http://www.ncbi.nlm.nih.gov/pubmed/17515901

Rouw, R., & Scholte, H. S. (2010). Neural basis of individual differences in synesthetic experiences. *The Journal of neuroscience : the official journal of the Society for Neuroscience*, *30*(18), 6205–13. Retrieved from http://www.ncbi.nlm.nih.gov/pubmed/20445046

Rueckert, D., Sonoda, L. I., Hayes, C., Hill, D. L., Leach, M. O., & Hawkes, D. J. (1999). Nonrigid registration using free-form deformations: application to breast MR images. *IEEE transactions on medical imaging*, *18*(8), 712–21. Retrieved from http://www.ncbi.nlm.nih.gov/pubmed/10534053

Salthouse, T. A. (1996). The processing-speed theory of adult age differences in cognition. *Psychological review*, *103*(3), 403–28. doi:10.1037/0033-295X.103.3.403

Salthouse, T. A. (2005). Relations between cognitive abilities and measures of executive functioning. *Neuropsychology*, *19*(4), 532–45. Retrieved from http://www.ncbi.nlm.nih.gov/pubmed/16060828

Salthouse, T. A. (2011). Neuroanatomical substrates of age-related cognitive decline. *Psychological bulletin*, *137*(5), 753–84. doi:10.1037/a0023262

Salthouse, T. A., Babcock, R. L., & Shaw, R. J. (1991). Effects of adult age on structural and operational capacities in working memory. *Psychology and aging*, *6*(1), 118–27. doi:10.1037/0882-7974.6.1.118

Schmierer, K., Wheeler-Kingshott, C. A. M., Boulby, P. A., Scaravilli, F., Altmann, D. R., Barker, G. J., Tofts, P. S., et al. (2007). Diffusion tensor imaging of post mortem multiple sclerosis brain. *Neuroimage*, *35*(2), 467–477. doi:10.1016/j.neuroimage.2006.12.010

Scholz, J., Klein, M. C., Behrens, T. E. J., & Johansen-Berg, H. (2009). Training induces changes in white-matter architecture. *Nature neuroscience*, *12*(11), 1370–1. Retrieved from http://www.pubmedcentral.nih.gov/articlerender.fcgi?artid=2770457&tool=pmcentrez&rendertype=abstract

Shaw, P., Greenstein, D., Lerch, J., Clasen, L., Lenroot, R., Gogtay, N., Evans, A. C., et al. (2006). Intellectual ability and cortical development in children and adolescents. *Nature*, *440*(7084), 676–9. doi:10.1038/nature04513

Smilek, D., Dixon, M. J., Cudahy, C., & Merikle, P. M. (2002). Synesthetic color experiences influence memory. *Psychological science*, *13*(6), 548–52. Retrieved from http://www.ncbi.nlm.nih.gov/pubmed/12430840

Smith, S. M. (2002). Fast robust automated brain extraction. *Human brain mapping*, *17*(3), 143–55. doi:10.1002/hbm.10062

Smith, S. M., Jenkinson, M., Johansen-Berg, H., Rueckert, D., Nichols, T. E., Mackay, C. E., Watkins, K. E., et al. (2006). Tract-based spatial statistics: voxelwise analysis of multi-subject diffusion data. *NeuroImage*, *31*(4), 1487–505. Retrieved from http://www.ncbi.nlm.nih.gov/pubmed/16624579

Smith, S. M., Jenkinson, M., Woolrich, M. W., Beckmann, C. F., Behrens, T. E. J., Johansen-Berg, H., Bannister, P. R., et al. (2004). Advances in functional and structural MR image analysis and implementation as FSL. *NeuroImage*, *23 Suppl 1*, S208–19. doi:10.1016/j.neuroimage.2004.07.051

Smith, S. M., & Nichols, T. E. (2009). Threshold-free cluster enhancement: addressing problems of smoothing, threshold dependence and localisation in cluster inference. *NeuroImage*, *44*(1), 83–98. doi:10.1016/j.neuroimage.2008.03.061

Song, S.-K., Sun, S.-W., Ju, W.-K., Lin, S.-J., Cross, A. H., & Neufeld, A. H. (2003). Diffusion tensor imaging detects and differentiates axon and myelin degeneration in mouse optic nerve after retinal ischemia. *Neuroimage*, *20*(3), 1714–1722.

Song, S.-K., Sun, S.-W., Ramsbottom, M. J., Chang, C., Russell, J., & Cross, A. H. (2002). Dysmyelination revealed through MRI as increased radial (but unchanged axial) diffusion of water. *Neuroimage*, *17*(3), 1429–1436.

Specht, K., & Laeng, B. (2011). An independent component analysis of fMRI data of grapheme-colour synaesthesia. *Journal of neuropsychology*, *5*(2), 203–13. Retrieved from http://www.ncbi.nlm.nih.gov/pubmed/21923786

Spiller, M. J., & Jansari, A. S. (2008). Mental imagery and synaesthesia: Is synaesthesia from internally-generated stimuli possible? *Cognition*, *109*(1), 143–51. Retrieved from http://www.ncbi.nlm.nih.gov/pubmed/18834583

StataCorp. (2009). Stata Statistical Software. College Station, TX: StataCorp LP.

Sternberg, R. J., & Rifkin, B. (1979). The development of analogical reasoning processes. *Journal of Experimental Child Psychology*, *27*(2), 195–232. Retrieved from http://dx.doi.org/10.1016/0022-0965(79)90044-4

Steven, M. S., Hansen, P. C., & Blakemore, C. (2006). Activation of color-selective areas of the visual cortex in a blind synesthete. *Cortex; a journal devoted to the study of the nervous*

system and behavior, *42*(2), 304–8. Retrieved from http://www.ncbi.nlm.nih.gov/pubmed/16683505

Takeuchi, H., Sekiguchi, A., Taki, Y., Yokoyama, S., Yomogida, Y., Komuro, N., Yamanouchi, T., et al. (2010). Training of working memory impacts structural connectivity. *The Journal of neuroscience : the official journal of the Society for Neuroscience*, *30*(9), 3297–303. Retrieved from http://www.ncbi.nlm.nih.gov/pubmed/20203189

Tang, Y.-Y., Lu, Q., Fan, M., Yang, Y., & Posner, M. I. (2012). Mechanisms of white matter changes induced by meditation. *Proceedings of the National Academy of Sciences of the United States of America*, *109*(26), 10570–4. Retrieved from http://www.ncbi.nlm.nih.gov/pubmed/22689998

Tang, Y.-Y., Lu, Q., Geng, X., Stein, E. A., Yang, Y., & Posner, M. I. (2010). Short-term meditation induces white matter changes in the anterior cingulate. *Proceedings of the National Academy of Sciences of the United States of America*, *107*(35), 15649–52. Retrieved from http://www.pubmedcentral.nih.gov/articlerender.fcgi?artid=2932577&tool=pmcentrez&rendertype=abstract

Taub, G. E., Keith, T. Z., Floyd, R. G., & Mcgrew, K. S. (2008). Effects of general and broad cognitive abilities on mathematics achievement. *School Psychology Quarterly*, *23*(2), 187–198. doi:10.1037/1045-3830.23.2.187

Taubert, M., Draganski, B., Anwander, A., Müller, K., Horstmann, A., Villringer, A., & Ragert, P. (2010). Dynamic properties of human brain structure: learning-related changes in cortical areas and associated fiber connections. *The Journal of neuroscience : the official journal of the Society for Neuroscience*, *30*(35), 11670–7. Retrieved from http://www.ncbi.nlm.nih.gov/pubmed/20810887

Thomason, M. E., & Thompson, P. M. (2011). Diffusion imaging, white matter, and psychopathology. *Annual review of clinical psychology*, *7*, 63–85. doi:10.1146/annurev-clinpsy-032210-104507

Tolhurst, D. J., & Lewis, P. R. (1992). Effect of myelination on the conduction velocity of optic nerve fibres. *Ophthalmic & physiological optics : the journal of the British College of Ophthalmic Opticians (Optometrists)*, *12*(2), 241–3. Retrieved from http://www.ncbi.nlm.nih.gov/pubmed/1408181

Turken, A. U., Whitfield-Gabrieli, S., Bammer, R., Baldo, J. V., Dronkers, N. F., & Gabrieli, J. D. E. (2008). Cognitive processing speed and the structure of white matter pathways: convergent evidence from normal variation and lesion studies. *NeuroImage*, *42*(2), 1032–44. doi:10.1016/j.neuroimage.2008.03.057

Voineskos, A. N., Rajji, T. K., Lobaugh, N. J., Miranda, D., Shenton, M. E., Kennedy, J. L., Pollock, B. G., et al. (2010). Age-related decline in white matter tract integrity and cognitive performance: A DTI tractography and structural equation modeling study. *Neurobiology of aging*, *33*(1), 21–34. doi:10.1016/j.neurobiolaging.2010.02.009

Vorísek, I., & Syková, E. (1997). Evolution of anisotropic diffusion in the developing rat corpus callosum. *Journal of neurophysiology*, *78*(2), 912–9. Retrieved from http://www.ncbi.nlm.nih.gov/pubmed/9307124

Ward, J., & Simner, J. (2005). Is synaesthesia an X-linked dominant trait with lethality in males? *Perception*, *34*(5), 611–23. Retrieved from http://www.ncbi.nlm.nih.gov/pubmed/15991697

Ward, J., Thompson-Lake, D., Ely, R., & Kaminski, F. (2008). Synaesthesia, creativity and art: what is the link? *British journal of psychology (London, England : 1953)*, *99*(Pt 1), 127–41. Retrieved from http://www.ncbi.nlm.nih.gov/pubmed/17535472

Waxman, S. G. (1980). Determinants of conduction velocity in myelinated nerve fibers. *Muscle & nerve*, *3*(2), 141–50. Retrieved from http://www.ncbi.nlm.nih.gov/pubmed/6245357

Wechsler, D. (1997). Weschler Adult Intelligence Scale - Third Edition. San Antonio TX: The Psychological Corporation.

Wechsler, D. (1999). The Wechsler Abbreviated Scale of Intelligence. San Antonio TX: The Psychological Corporation.

Weiss, P. H., & Fink, G. R. (2009). Grapheme-colour synaesthetes show increased grey matter volumes of parietal and fusiform cortex. *Brain : a journal of neurology*, *132*(Pt 1), 65–70. Retrieved from http://www.ncbi.nlm.nih.gov/pubmed/19028762

Weiss, P. H., Zilles, K., & Fink, G. R. (2005). When visual perception causes feeling: enhanced cross-modal processing in grapheme-color synesthesia. *NeuroImage*, *28*(4), 859–68. Retrieved from http://www.ncbi.nlm.nih.gov/pubmed/16111898

Wendelken, C., & Bunge, S. A. (2010). Transitive inference: distinct contributions of rostrolateral prefrontal cortex and the hippocampus. *Journal of cognitive neuroscience*, *22*(5), 837–47. Retrieved from http://www.pubmedcentral.nih.gov/articlerender.fcgi?artid=2858584&tool=pmcentrez&rendertype=abstract

Wendelken, C., Chung, D., & Bunge, S. a. (2011). Rostrolateral prefrontal cortex: Domain-general or domain-sensitive? *Human brain mapping*, *00*. doi:10.1002/hbm.21336

Wendelken, C., O'Hare, E. D., Whitaker, K. J., Ferrer, E., & Bunge, S. A. (2011). Increased Functional Selectivity over Development in Rostrolateral Prefrontal Cortex. *Journal of Neuroscience*, *31*(47), 17260–17268. doi:10.1523/JNEUROSCI.1193-10.2011

Williams, R. L. (2000). A note on robust variance estimation for cluster-correlated data. *Biometrics*, *56*(2), 645–6. Retrieved from http://www.ncbi.nlm.nih.gov/pubmed/10877330

Woodcock, R. W., Mather, N., & McGrew, K. S. (2001). *Woodcock-Johnson III*. Itasca, IL: Riverside Publishing.

Woolrich, M. W., Jbabdi, S., Patenaude, B., Chappell, M., Makni, S., Behrens, T. E. J., Beckmann, C. F., et al. (2009). Bayesian analysis of neuroimaging data in FSL. *NeuroImage*, *45*, S173–86. doi:10.1016/j.neuroimage.2008.10.055

Yakovlev, P., & Lecours, A. (1967). The myelogenetic cycles of regional maturation of the brain. In A. Minkowski (Ed.), *Regional development of the brain in early life* (pp. 3–70). Oxford: Blackwell Scientific.

Yaro, C., & Ward, J. (2007). Searching for Shereshevskii: what is superior about the memory of synaesthetes? *Quarterly journal of experimental psychology (2006)*, *60*(5), 681–95. Retrieved from http://www.ncbi.nlm.nih.gov/pubmed/17455076

Zatorre, R. J., Fields, R. D., & Johansen-Berg, H. (2012). Plasticity in gray and white: neuroimaging changes in brain structure during learning. *Nature Neuroscience*, *15*(4), 528–536. doi:10.1038/nn.3045

Zhang, J., Jones, M., DeBoy, C. A., Reich, D. S., Farrell, J. A. D., Hoffman, P. N., Griffin, J. W., et al. (2009). Diffusion tensor magnetic resonance imaging of Wallerian degeneration in rat spinal cord after dorsal root axotomy. *The Journal of neuroscience : the official journal of the Society for Neuroscience*, *29*(10), 3160–71. Retrieved from http://www.pubmedcentral.nih.gov/articlerender.fcgi?artid=2683764&tool=pmcentrez&rendertype=abstract

Zhang, Y., Brady, M., & Smith, S. M. (2001). Segmentation of brain MR images through a hidden Markov random field model and the expectation-maximization algorithm. *IEEE transactions on medical imaging*, *20*(1), 45–57. doi:10.1109/42.906424

van Leeuwen, T. M., Petersson, K. M., & Hagoort, P. (2010). Synaesthetic colour in the brain: beyond colour areas. A functional magnetic resonance imaging study of synaesthetes and matched controls. *PloS one*, *5*(8), e12074. Retrieved from http://www.pubmedcentral.nih.gov/articlerender.fcgi?artid=2919410&tool=pmcentrez&rendertype=abstract